


# Measurement-induced physics and stochastic dynamics in systems of single-body quasiparticle and many-body microscopic cases

Chen-Huan Wu <sup>1,\*</sup>

<sup>1</sup>*College of Physics and Electronic Engineering,  
Northwest Normal University, Lanzhou 730070, China*

In this article, we focus on measurement-induced physics and stochastic dynamics in the systems of single-body quasiparticle and many-body microscopic cases. In the former case, it shows a smooth evolution from a non-Gaussian (Poisson or binomial distribution) with local dephasing to a Gaussian with global dephasing (quantum microscopic to classical macroscopic) where in late time there is a global symmetry that consists of exponentially many pure states due to the suppressed (stochastic) fluctuation and heating; In the latter case, it shows exponentially many distinct (Krylov) sectors due to the fragmentation and dynamical constrain on Hilbert-space. A gapless-to-gapped transition ((sub)volume law to area-law) during evolution is evident for the former case, where, however, the asymptotic approaching area-law scaling (system-size-independence) even appears in early time with the increasing system-size toward infinity. A novel purifying lasting for a short time is found in the early stage of the former case, during which there is long-range power law decay and scrambling before the Lieb-Robinson bound. Meanwhile, in the latter case, local non-Gaussian interactions (with a large power-law exponent) are present, maintaining an invariant gapless feature. Except a comprehensive study for the both cases, our scheme avoid the interaction effect as well as the selections on measured states due to the measurement apparatus, and thus easier evaluatin on the expectations of non-Hermitian observables.

## I. INTRODUCTION

It has been studied that a pair of coupled identical Sachdev-Ye-Kitaev (SYK) models with complex fermions provide globally chaotic systems which allowing the quantum mutual information to traverse through the wormhole[1], where the robust ergodicity against the localization is supported by the revival oscillations between the two chaotic subsystems[1, 2]. Similarly, a periodic initial state revivals in a many-body system indicate the nonthermal feature in the quench dynamics up to long-time limit (infinite temperature or high energy density)[22, 142, 172], which is distinct to the conventional many-body scars. The non-Hermitian dynamics can arises from the quantum dissipation or continuous measurement together with postselected trajectories (exponentially costly[28, 158]). The non-Hermitian skin effect with finite dissipation (imaginary) gap in complex spectrum shows area-law entanglement scaling. The skin effect is caused by the nonreciprocal dissipation and thus suppressing the entanglement diffusion. Despite sharing the boundary localization, the edge burst[57] additionally require closing dissipative gap[28, 53, 54], origin from a universal bulk-edge scaling relation. Moreover, the multi-partite entanglement can be effectively manipulated through the non-Hermitian (asymmetry) coupling. Note that in this article, for skin effect, we only refer to the nonreciprocal one, i.e., excluding the reciprocal induced by  $Z_2$ -type symmetry[61, 64], and for coherence, we only refer to the one happen in non-Markov case, such that the coherence field (pattern) corresponding to a closed system in a pure state, instead of the global conservation (topological invariance). In non-Hermitian (open) system, there is unidirectional disentangling due to the coupling to the external disorder. Then there is possibly be infinite number of bound states (in gapped regime) discretically, among which are mutually uncorrelated and the level statistics follows Gaussian ensemble (random matrices). The only way to reveal such external disorder (or non-Hermitian perturbation) is to continuously monitor a individual quantum trajectory, which is a separable pure state (corresponding to a rank-1 subspace) with the continuously measured outcomes be postselected. Here the "individuality" is guaranteed by conditioning the evolution to the absence of quantum jump (sudden change of state) as well as the exceptional point[12–15]. Such individual trajectory subject to unitary evolution (by certain Hermitian operator  $H$ )  $|\psi(t)\rangle = \frac{e^{-iHt}|\psi_0\rangle}{\|e^{-iHt}|\psi_0\rangle\|}$  is conditioned during the continuously measurement and thus support the long-range entanglement, while the repeated local measurement (monitoring) will suppress the short-range

---

\* chenhuanwu1@gmail.com

entanglement[39, 44] by alternating the random unitaries and introducing the quantum jump processes accompanied by the density fluctuation.

In this article, instead of exploring the measurement-induced transition, we study the two extreme cases, the limit of weak but continuous measurement and strong but sparse measurement, such that the measurement apparatus plays little role in our scheme. This also provides great convenience in measuring the non-Hermitian observables, where the perturbations-induced imaginary part due to the measurement apparatus can be ignored and thus the preselection on measurement basis is needless. In other word, the uncertainty and randomness are not due to the selections by measurement apparatus, which mean the Green function here does not contains a self-energy term. In many-body microscopic case, the projective measurement suppress the long-range entanglement but does not cause the selections on measured states due to the effect of unique Markovian bath. Another reason is that we choose a time-independent basis  $\langle \rho_0 | \rho_0 \rangle$ . Consequently, the mapping  $|\rho_0\rangle \rightarrow |\rho'_0\rangle$  does not cause any new conservations. This indeed reflects the existence of response to the global quench in many-body microscopic case, just like the complete thermal state in late stage of single-body quasiparticle case, i.e., the common characteristic between the Markovian system in single-body quasiparticle case and the unique Markovian bath in many-body microscopic case. These are proved by the expectation (Green function) and variance of non-Hermitian observable[180] as well as the Jensen-Shannon divergence (JSD) in this article.

## II. EFFECT OF MEASUREMENT IN BIPARTITE CONFIGURATION

Lindblad master-equation[16] for dissipative Markovian process, consisting of a coherent interacting term and a local dissipation term, and where measurement outcomes are averaged out, is most appropriate[13–15, 17] in the absence of detection of quantum jumps, in which case the system jumps to the state  $|\psi(t+dt)\rangle = L\sqrt{\gamma dt}|\psi(t)\rangle$  with a probability of  $\gamma dt \langle \psi | L^\dagger L | \psi \rangle$  ( $L$  is the jump operator and  $\gamma$  is the measurement rate). In this case with the presence of non-Hermitian skin effect, we can suspect the unique external disorder help the system to retain initial information, in opposite with the quasi-particle effect. This corresponds to the densities of the class of many-body microscopic ( $mm$ )  $\rho_{mm;\{i\}}$ , which is a Hermitian matrix and characterize the robustness of initial state revival as well as the bulk disentangling liquid which prohibits the diffusion of quantum mutual information (correlation) among the whole system globally. The counterpart of  $\rho_{mm;\{i\}}$  is defined as  $\rho_{sq;\{i\}}$ , which is a non-Hermitian matrix. Here the subscript  $sq$  refers to single-body quasiparticle. For  $\rho_{sq}$ , the non-Hermitian skin effect is absent, and there is delocalization as well as thermalization due to the non-Hermiticity induced by  $\mathbb{Z}_2$ -type field, before the thermal equilibrium where the system becomes exactly Hermitian and local with respect to the unique environmental disorder (thermal bath) which should be distinguished from the above-mentioned external disorder for  $\rho_{mm}$ . Also, for  $\rho_{sq}$ , there is a diffusion (nonreciprocal dissipation) of quantum mutual information (carried by heavier carrier) among the whole system globally, and thus there will not be disentangling liquid within the bulk but only be a single disentangling boundary. Consequently, such correlation is system-size-dependent, or, extensive. This meets the label of single-body quasi-particle whose lifetime entirely controlled by the unique environmental disorder, and it is impossible for the multi-bound-states to appear like the case of  $\rho_{mm}$ . Importantly, even the non-Hermitian density  $\rho_{sq}$  is diagonalizable due to the existence of non-defective degeneracy (NDD). While for the non-Hermitian operators that contains only the defective degeneracy, it becomes nondiagonalizable at certain momentum termed exceptional point. This means the set of eigenvectors that support non-defective degenerate span a full Hilbert space, in contrast to the defective degenerated one. Importantly, the non-defective degeneracy of  $\rho_H$  preclude the symmetry-protected many-body localization and guarantees the global symmetry (chaos), thus its complex eigenenergies is different from that of a quasiparticle in a system with topologically enclosed exceptional point, such that its imaginary part (inversed lifetime) is directly determined by the unique environmental disorder from thermal bath (unlike the regular quasiparticles induced from a quantum jump process), and we further found that its real part of eigenenergies correlated (uncorrelated) with the imaginary part outside (inside) the NDD block. While for regular quasiparticles the imaginary part of eigenenergies close and away from the exceptional points are always related to different sources. It is found that the topologically stability of exceptional points requires two or higher dimensions for a nontrivial topological index and can only be created or annihilated in pairs[82], thus the defectively-degenerated system containing exceptional points requires additional dimension compares to the non-defectively degenerated one. This is in consistent with the NDD eigenvectors constructed in our configuration, where the forward-scattering-like[172] eigenvectors in degenerated region preventing the formation of many-body localization, and the superpositions of NDD eigenvectors form a null-(sub)space whose correlation inside is extensive and thus guaranteeing the global symmetry. Such extensive correlation, or the dependence on the size of global system, is in analogy with the topological invariant with noncontractible path in momentum space[82], unlike the

contractible path for a non-Hermitian system with defective degeneracy (exceptional points enclosed by the path).

In thermodynamic limit with projective measurement, the correlations as well as entanglement entropy is bounded (unbound) for ergodic (coherent) system, as detailed below in  $sq(mm)$ -case.

### A. Long-range entanglement and thermal equilibrium steady state

The trajectory of discontinuous conditioned stochastic evolution with quantum jumps becomes the continuous diffusive quantum trajectory in the limit of strong dissipation with an infinitesimal Wiener increment (the Markov limit which invalidates the photon detection by white noise). The Wiener increment has a zero mean over the evolution described by stochastic Schrödinger equation instead of Lindblad master equation. Such a stochastic continuous measurement (which initially acts locally on the quantity like occupation number or spontaneous emissions in an optical lattice) mainly contributed by the Wiener process (Brownian motion) with the transition from jump evolution (stochastic) to diffusive evolution (Ito stochastic)[34, 41, 45, 50, 51, 90, 91]. This also accompanied by a transition from ballistic propagation (spreading) of quasiparticle (entanglement) to diffusive spreading of, e.g., energy. Despite initially the discontinuous local measurements on the conditioned evolution of jumps (i.e., low emission rate in which case the Born-Markovian approximation is valid) will hinder the thermalization (decoherence), the raised emission (dissipation) rate or strongly diffusive transport through the collision-induced quasiparticles[50, 51] (or other non-local carriers), guarantee the thermalization in final stage[28, 34, 91]. The ballistic (and uncorrelated) spreading of informations is suppressed by the local measurements as well as the unitary evolution[45, 46]. The continuous homodyne or heterodyne non-projective measurements are of such detection[34, 41, 91]. In some cases, the white noise limit leads to maximally mixed state with maximal entanglement (e.g., infinite two-point correlation[43, 58]). While the local projective measurements will suppress the unitary-evolution-induced short-range entanglement, the local projective measurements with unitary evolution can contribute to the generation of long-range entanglement or a global (topological) symmetry[44] at low-temperature, and being area-law scaling for steady state. In the other hand, a mode involving mutually commuting particles (repeated action) among a long-range[39, 51] that storing the same informations, generally has long-range entanglement, like the nonlocal condensate with global phase locking[51], and nonlocal measurement is applied for such information. In fact, long-range (short-range) entanglement usually emerges in local (thermal) state with area (volume) law scaling entanglement[39, 44, 81], like the Bose-Einstein condensate dark pure state (non-Abelian anyons). Note that here the nonlocal condensate is out-of-thermal-phase superposition coherence. Such mode applied in Born-Markovian approximation implies the absence of bound state or coherence and the presence of weak-dissipation-coupling-induced spontaneous emission and collision. In the absence of spontaneous emission the entanglement is generated by the global incoherence which is exactly of the non-Hermitian picture depicted in the early stage of  $sq$ -case; An circuit realization is achieved through the global incoherence noise which acts uniformly on each every qubit[55]. While the above-mentioned decoherence case is depicted in the late-stage of  $sq$ -case.

While approaching the continuous-limit leads to measurement-induced entanglement transition in single-particle picture with area-law saturating entanglement and maximally mixed steady state with maximal measurement (or dissipation) rate upto thermodynamic limit, a volume-to-area transition is visible at finite time for the discontinuous measurement (without unitary conditional feedback), termed as pseudo-skin effect under open boundary condition[52, 56]. Such pseudo-skin effect as well as dynamical entanglement transition is manipulated by the time step of quantum jump, instead of the disorder, conditional feedback or measurement.

Except the measurement-induced entanglement transition, there is another kind of suppression on long-range entanglement, which is by the conditional feedback (locally operates on the unpostselected trajectories) with the trajectory-average consistent with the Lindblad master-equation approach[12, 13, 28]. Such feedback-induced skin effect can happen in both the noninteracting (free fermion) system and chaotic interacting system, and requires continuous measurements (white noise limit), thus results in unconditioned diffusive trajectories with short-range area-law entanglement and suppress the measurement-induced entanglement transition (i.e., from diffusive logarithmic scaling entanglement to saturating one)[39, 52].

Similar to the skin effect of non-Hermitian system feedback-induced skin effect results in area-law entanglement for the steady states concentrate at edge, and there may even be multiple edges for unitary dynamics. Differently, in the absence of spin effect ( $sq$ -case), each subsystem thermalizes following the volume law scaling before approaching the steady state which is extensive with subsystem size. Thus these are two distinct kinds of disentangling.

The repeated local measurement with local feedback cause the averaging over the coherently superposed trajectories (nonindividual). Specifically, at generic unital quantum channel the identity operator becomes stationary with short-range entanglement. For such (passive) measurement with unconditioned dynamics, there is an average

on the trajectory-ensemble level, and essentially, this average is a coherent superposition instead of a statistical mixture since the latter equivalent to a ensemble of identical copies (individual trajectories) each in a pure state. Comparing the Lindbladian master equation with the non-Hermitian Hamiltonian, the conditional feedback only operates on the trajectories deviated from postselection, i.e., the quantum jump processes (collective dissipation with each individual quantum trajectory subject to stochastic loss events),  $\sum_i \gamma_i L_i \rho L_i^\dagger$  with  $\gamma_i$  and  $L_i$  the dissipation rate and jump measurement operator, respectively. The quantum channel map to itself when  $[\rho, (\sqrt{\gamma_i} L_i)^\dagger] = 0$ , such that  $\sum_i (\sqrt{\gamma_i} L_i) \rho (\sqrt{\gamma_i} L_i)^\dagger = \rho$ . While system temperature can be affected by the measurements only when  $[H, (\sqrt{\gamma_i} L_i)^\dagger]$  is nonzero[80, 87].

### B. Short-range entanglement and nonequilibrium steady state

For *mm*-case the short-range entanglements (with nonlocal measurement) is necessary where there are coherences with weak dissipation (i.e., the non-Markovian dynamics with robust memory effect) and finite-time thermalization (in terms of energy spectrum, this can be evidenced by the gapped structure and variant number of bound states[10, 47]). Thus different to the above cases of density-bath (decoherenced and disentangled), the strong system-bath coupling produce bound states with high fidelity. Another phenomenon in the limit of closed system is tunneling as a stochastic process where the non-perturbational resonance at some certain local spatial sites is overwhelming compares to others due to the statistical fluctuations of the on-site disorder. This give rise to the non-Hermiticity through the mixing of non-adjacent eigenstates and all-to-all coupling as can be evidenced by the complex eigenenergies[13, 56, 173].

Note that the all-to-all limit (Dicke limit) corresponds to the lowest effective dimension (where, e.g., the long-range hopping prompt the homogenization in density distribution), or infinitely large system size, where the open boundary condition and periodic boundary condition produce similar dynamics, similar to the case of strong-disorder-induced dynamically stable non-Hermitian many-body localization with the evolution dominated by area-law scaling. Also, in all-to-all limit, the localization length as well as the density imbalance of the particle distribution becomes nonextensive. Under periodic boundary condition, there is uniform density distribution in late-time steady state[56] (without incompressible density or domain structure in spatial space). While in the presence of skin effect, which is compatible with many-body nature as long as it is not in the all-to-all limit and involves finite interacting effect (dissipation), i.e., in the nonreciprocity limit of Hatano-Nelson model with biased (imbalanced) density distribution, the entanglement phase transition only exists for weak disorder under open boundary condition before it reaches the late-time steady state.

Through Loschmidt echo, a robust initial siate fidelity reflecting such high-overlap-induced large amplitude (be independence of bath). This should be distincted from the amplified local oscillator in coherence field in homodyne limit with continuous measurement, where the coherence is tightly related to the bath (infinite photodetection rate) and obviously not a closed system. The complex coherence pattern as well as the emergent bound states can be visualized by the Loschmidt echo, as detailed below. Additionally, the conserved quantities (like the bound state) exhibit linearly (in Hilbert space dimension) large lifetime (relaxation time) and thus logarithmically slow the transport[48] and lower the correlation[43], deviate away from the white-noise (Markov) limit.

## III. TRACE DISTANCE AND MAJORIZATION

The off-diagonal fluctuation, which plays a subleading role in ETH) vanishes in long-time limit, and thus the off-diagonal elements exponentially small in system size. A completely thermalized final state has zero off-diagonal part, and can be described by a gapless phase[10, 19] As a result, the deviation of the density from the one in diagonal ensemble,  $\rho(t) - \rho_d = |\psi(t)\rangle\langle\psi(t)| - \sum_i |\langle i|\psi_0\rangle|^2 |i\rangle\langle i|$ , satisfies

$$(\rho(t) - \rho_d)^2 = \sum_{i \neq j} \langle \psi_0 | i \rangle \langle j | \psi_0 \rangle e^{i(E_i - E_j)t} |j\rangle\langle i| \sum_{k \neq l} \langle \psi_0 | k \rangle \langle l | \psi_0 \rangle e^{i(E_k - E_l)t} |l\rangle\langle k|, \quad (1)$$

whose long-time average reads

$$\begin{aligned} \langle (\rho(t) - \rho_d)^2 \rangle_t &= \sum_{i \neq j} \langle \psi_0 | i \rangle \langle j | \psi_0 \rangle |j\rangle \langle i| \langle \psi_0 | j \rangle \langle i | \psi_0 \rangle |i\rangle \langle j| \\ &= \sum_{i \neq j} |\langle \psi_0 | i \rangle|^2 |\langle j | \psi_0 \rangle|^2 |j\rangle \langle i| \langle i \rangle \langle j| = h^2 - \sum_i |\langle \psi_0 | i \rangle|^4 (|i\rangle \langle i|)^2, \end{aligned} \quad (2)$$

where  $h = (\sum_{ij} |\langle \psi_0 | i \rangle|^2 |\langle j | \psi_0 \rangle|^2 |j\rangle \langle i| \langle i \rangle \langle j|)^{1/2}$  is a Hermitian full-rank matrix. The variance of eigenvalues of  $h$  is nearly three times of that of  $h^2$ . Note that  $h \neq \rho_{nd}$  with  $\rho_{nd}$  be a idempotent matrix  $\rho_{nd} := \sum_{ij} \langle i | \psi_0 \rangle \langle \psi_0 | j \rangle |i\rangle \langle j|$ , but  $\text{Tr} h^2 = \text{Tr} \rho_{nd}^2 \equiv 1$ . The last term in above relation satisfies  $\sum_i |\langle \psi_0 | i \rangle|^4 (|i\rangle \langle i|)^2 = \rho_d^2$ , where the coefficient  $\text{Tr}(\rho_d^2) = \sum_i |\langle \psi_0 | i \rangle|^4 (< 1 = \sum_i |\langle \psi_0 | i \rangle|^2)$  defines the purity and tell the deviation of  $\rho_d$  from a pure state. The corresponding traces satisfy

$$\langle \text{Tr}[(\rho(t) - \rho_d)^2] \rangle_t = \text{Tr}[(\rho(t) - \rho_d)^2] (\forall t) = \text{Tr} h^2 - \text{Tr} \sum_i |\langle \psi_0 | i \rangle|^4 (|i\rangle \langle i|)^2 = 1 - \sum_i |\langle i | \psi_0 \rangle|^4 > 0. \quad (3)$$

While  $\text{Tr}(\rho(t) - \rho_d) = 0 (\forall t)$ , which corresponds to the vanishing fluctuation (off-diagonal part) for the system of  $\rho_H$ . For the *sq*-case, there without any atypical state (nonthermal and nonergodic) and the initial state revival (i.e., back to the nonequilibrium state) cannot be found, which corresponds to the case that the subsystems of the nonequilibrium state be a nearly vanishing fraction of the total states. This is a scenario much more closer to equilibrium compares to the one discussed in Ref.[19]. Considering a bipartition of the restriction-allowed states into the system part and environmental part, smaller the dimension of system part  $d_s = (\sum_i |\langle i | \psi_0 \rangle|^4)^{-1}$  (inversed purity) is, shorter the distance between  $\rho(t)$  and  $\rho_d$ . Reminiscent to the distance between a state of very small subsystem  $\rho_S = \text{Tr}_E \rho_{\text{pure}}$  and the canonical state  $\rho_{\text{can}} = \langle \rho_S \rangle = \text{Tr}_E \rho_{\text{mix}}$ . For a global restriction, each pure state of the system becomes close to the maximally mixed state  $\rho_{\text{can}} = \mathbf{I}_s/d_s$ [21–23]. The process of such proximity can be realized gradually by enlarging the kinematical restriction to the size as large as the universe. However, we found that such averaging feature can be realized without the exponentially small dimension of subsystem compares to the rest part, as long as there contains a NDD nullspace, i.e., the eigenvector set span a full Hilbert space.

While for the many-body microscopic system (the *mm*-case), each subspace, which is also the smallest subsystem, is spanned by a rank-1 pure state, then we found that each smallest subsystem is evolved to the equilibrium which can be seen from the stable pattern of fidelity (), and such equilibrium state does not thermalized with respect to the environmental disorder (thermal bath) and be able to coherent with other subsystems (in arbitrary size). Thus final equilibrium state behaves as a mixed state governed by non-Abelian symmetry, and this is in agree with the statement of Refs.[19, 21, 30]: For a sufficiently small subsystem (thus a small fraction of the total states) almost every pure state is locally indistinguishable from the mixed state with entangling (whose trace over the environment part is a thermal canonical state). In other word, the massive entanglement between the very small subsystem and its effective environment render the proximity from a pure state to maximally mixed state with maximal entanglement, and this is also related to the majorization of pure states[25], e.g., the arbitrary state with probability distribution away from uniform (equilibrated) distribution majorize the maximally mixed state[24, 25] which has a largest entropy. We found that, this characteristic of small subsystem can be seen from the subsystems of the NDD regime, such that arbitrary subspaces or subsystems of the NDD regime exhibit no coherence with the arbitrary piece of the rest part of global system. This can be seen from the thermal character and the persistive initial-state revival (large recurrence). Importantly, in our configuration, it requires not exponentially large dimension of the environmental part compares to that of the subsystem. This can also be understood as a large effective dimension is hidden in a system containing the NDD.

A pure state can be entangled or unentangled, depending on it is separable or not. This correspond to the two kinds of subspaces (complex density matrices) of the *mm*-case or *sq*-case (in different bases), where the former are unentangled while the latter are entangled. In other word, there is a subjective lacking of information regarding the global system for the pure states of *mm*-case compares to the *sq*-case, The regain of such subjective information (weight on each subspace) is possible for small enough subsystem[21], or by move to the NDD nullspace (where the eigenstates become real and the corresponding subsystems therein become Hermitian). Thus, such subjective information is essential for the entanglement, and as a result, the entanglement is possible to be preserved even in Gibbs stationary states of some non-local Hamiltonians, whose quantum channel can be artificially designed[26]. In bipartite configuration, a bipartite pure state reads  $|\psi\rangle = \sum_i^D \lambda_i |\psi_S\rangle \otimes |\psi_E\rangle$ , and the reduced states are  $\rho_{S(E)} = \text{Tr}_{E(S)} |\psi\rangle \langle \psi| = \sum_i^D |\lambda_i|^2 |\psi_{S(E)}\rangle \langle \psi_{S(E)}|$ . The pure bipartite state is maximally entangled, if the reduced density



matrix on either system is maximally mixed, and the corresponding Schmidt coefficients be  $\lambda_i = \sqrt{1/D}$  and the purity of each subsystem is  $\sum_i |\lambda_i|^4 = 1/D$ . In opposite case, the separable pure states has  $|\lambda_i| = \delta_{i,1}$  the each reduced system as well as their separable product is pure state, such that  $\rho_S \otimes \rho_E = |\psi\rangle\langle\psi|$ . In sq-case, a entangled pure state  $|\psi_1\rangle$  is possible to be transformed into another state entangled  $|\psi_2\rangle$  as long as it satisfies  $\text{Tr}_S|\psi_1\rangle\langle\psi_1| \prec \text{Tr}_S|\psi_2\rangle\langle\psi_2|$  (we denote the eigenvalues of these two matrices made up the vectors  $|E_1\rangle$  and  $|E_2\rangle$ , respectively). This transformation can be implemented by the Local Operations assisted by Classical Communication (LOCC)[24, 27]: a single local measurement on the system part and a nonlocal unitary operation on the environmental part. Then it is guaranteed that  $|E_1\rangle \prec |E_2\rangle$ , i.e., the state  $|E_2\rangle$  majorize the state  $|\psi_1\rangle$  since the latter is disordered stronger than the former, (such that their entropies  $S(|\psi_2\rangle) < S(|\psi_1\rangle)$ ).

For the densities of *mm*-case, for *i*-th subspace,  $|E_i\rangle = (0, 0, \dots, 0, 1)^T$ .  $|E_{i,j,k,\dots}\rangle \prec (0, 0, \dots, 0, 1)^T$  where *i, j, k, ...* denote the distinct subspaces, and this majorization relation is valid as long as it include more than one subspace. Specifically, there is super-majorization for  $|E_{i,j,k,\dots}\rangle$  including all the subspaces, such that  $\sum_i^{D-1} E_i(\rho_{mm;c_1}) < \sum_i^D E_i(\rho_{mm;c_1}) = 1$ . This is consistent with the unentangled subspaces of the *mm*-case, as the coherence between the arbitrary subsystems outside the NDD regime produce the non-local symmetries (bound state in infinite amount) where the induced short-range entanglement overwhelming the local measurement-induced disentangling (volume law to area law transition; which appears in the *sq*-case).

## IV. ENTANGLEMENT AND MEASUREMENT

### A. *sq*-case

The *sq*-case corresponds to the monitored system with random quantum jumps (discontinuous), where the measurement results are unknown due to the average in trajectory ensemble. Also there are long-range entanglements with adaptive dynamics in this case, before the averaged state is being completely thermalized (dephased), with respect to measurement basis, into the Hermitian local states.

Thus the entanglement transitions from volume law to area law (mainly refer to the one induced by the skin effect) is more significant for the conditioned trajectories, since the entanglement is contingent upon the measurement outcomes[36] and diminished once the measurement record lost.

Considering the trajectory-averaged entanglement, the reduced density matrix on *i*-th eigenvalue  $R_i = \begin{pmatrix} \lambda_i & \nu \\ \nu^* & 1 - \lambda_i \end{pmatrix}$  always has the eigenvalues majorize its diagonal elements as long as the off-diagonal element is nonzero ( $\nu \neq 0$ ):  $(\frac{1}{2}(1 + \sqrt{(1 - 2\lambda_i)^2 + 4\nu\nu^*}), \frac{1}{2}(1 - \sqrt{(1 - 2\lambda_i)^2 + 4\nu\nu^*})) \succ (\lambda_i, 1 - \lambda_i)$ . The classical Shannon entropy provides a upper bound on the entanglement entropy,  $-\lambda_i \ln \lambda_i - (1 - \lambda_i) \ln(1 - \lambda_i) \geq -\text{Tr}[R_i \ln R_i]$ . Note that for Shannon entropy, the eigenvalues always be normalized to be  $\sum_i \lambda_i = 1$ . This entropy uniquely determined by  $\lambda_i$  is also called Boltzmann one-body entropy[35], which referring to the single-particle Hilbert space. As also reflected by the Loschmidt echo, the free-particle in single-particle picture exhibit much weaker ability in quantum information memory, due to the lacking of interaction (with reservoirs).

The *sq*-case and *mm*-case reflect the entanglement (sub)additivity and symmetry additivity, respectively. As a result, the former has a much larger measurement rate, and exhibits more pronounced randomness.

The disentangling effect induced by Abelian symmetries, like  $Z_2$  gauge symmetry or  $U(1)$  symmetry, appear only in the *sq*-case after long time evolution. Although such Abelian symmetrie is fragile to the dissipation processes[37], fluctuation of order parameter, charge diffusion[38], or noisy-driven biased random walk, the symmetry breaking is avoided by the effectively low-dimensional structure of the eigenspace where the eigenstate coalescence (as happen in delocalized phases) is absent. In other word, the non-defective degenerate structure in *sq*-case effectively avoid the dynamical instability of the delocalized eigenstates (in the early stage of evolution), and consequently there is no emergent symmetry sectors and entanglement between each subspace is robust. As the non-Hermiticity dominate in the early stage of (non-unitary) evolution, the nonlocal measurements on the individual conditioned trajectories can generate entanglement[36, 39], but different to the kind of adaptive dynamics as mentioned above (which is of the Hermitian case).

While before long-time limit, there is global quantum correlation (i.e., global entangling) throughout the whole system, where there is continuous non-Abelian symmetries, like the  $SU(2)$  symmetry, and thus allowing the long-range entanglement and logarithmically large entanglement. Typically, this is the case for closed quantum system, where the quantum mutual information diffuse throughout the whole system during evolution, with extensive correlation (or entanglement), and finally realize thermalization with the vanishing off-diagonal fluctuation and non-Hermiticity. Opposite to this, the *mm*-case corresponds to the discrete non-Abelian symmetry, where there is

(relatively) short-range entanglement with local unitaries. As a typical example, for the quantum jump term as mentioned above which describes the measurement with an unknown result (to be averaged out), it turns to be a strongly symmetric channel if the jump operator can be decomposed into a form that is diagonal in the space of each irreducible representation (irrep) and not on the multiplicity space[30]. Thus it allows both the cases of non-Abelian symmetry and Abelian symmetry, which has more than one and only one state in each irrep, respectively.

In the presence of large dissipation and decoherence arising by the (weak) system-bath interaction, the entanglement growth is suppressed such that the dephased states have area law scaling due to the ergodicity, and the single-particle-picture is well preserved by low-effective-dimensionality of the eigenspace as mentioned above. For an arbitrary subsystem which must behave as an open quantum system, the rest part can be treated as a thermal (or Gaussian) environment which can be expressed as a product of all the (commuting but long-range entangled) thermal states therein. Due to the definite eigenvalue for each subspace, the operator expectation, which is a linear quantity (linear on the time-dependent stochastic states), can be retrieved from a master-equation[39, 40]. One of the monitoring protocols for weak measurement is the phase locking between adjacent sites[39] which is consistent with the low-effective-dimension structure, and low-effective-dimensionality throughout the whole system. Similar to the special structure of the NDD eigenvectors, the phase locking preventing the many-body localization by breaking the local  $U(1)$  symmetry. Note that the phase locking here is of the Markov process accompanied by the spontaneous emission (quantum jump). Consistent with the fact that the phase locking is closely related to the long-range entanglement and Born-Markovian approximate (which is applicable in the case of weak system-bath coupling and without bound state[39, 47]), there is a strong dependence on the subsystem size for the entanglement entropy growth, which moves to the area law scaling in the regime where the dephasing dominates (with strong system-bath coupling).

In *sq*-case, the thermalization is allowed by the diffusive spreading of initial state information (or correlations) over the entire system (up to long-time limit) and meanwhile small local subsystems are possible to lose the memory about initial information and relax to thermal state under weak disorder. This corresponds to the non-local measurement, e.g., the measurement ideally affects all the bonds in a spin chain model, which will lead to superballistic spreading (of entanglement or quantum information) under nonunitary evolution[46]. Such superballistic spreading has a faster-than-linear entanglement growth, which appears in the initial stage of spreading[50] where there is equivalent bipartition with maximal thermodynamic entropy. While in the presence of nonlocal measurement and unitary evolution, there is ballistic spreading with linear entanglement growth following the volume law. Distinct to the former, the ballistic spreading involving the process with information spread from one heavy carrier to another heavy carrier through the carrier-carrier interaction, such that the entanglement is generated between those carriers (with information scrambling). An example of such carrier (a local degree of freedom) satisfying the volume scaling law is the spin[15, 50]. In contrast to nonlocal measurement, the local measurement will not prohibit the global thermalization, whose impact is exponentially localized[49]. Importantly, the non-local measurement causes the ballistic entanglement spreading (and diffusive entanglement spreading throughout the system in the late-time stage [15, 50]) in *sq*-case where the perturbation from local projective measurement is avoided by the effective single-particle picture, coexist with the diffusive energy (or information carriers) transport throughout the whole system. Except the continuous level distribution[92], we further found that the equally-spaced eigenvalues (of the thermal states) also reveals the invalidity of perturbation theory. In this case, the only local observable is the total energy, thus there is no ballistic transport in terms of ballistically traveling quasiparticles[50], like photon is absent, and the only way for energy transport is diffusion (through strong scattering).

## B. *mm*-case

The *mm*-case corresponds to a constrained Hilbert space with extensive entanglement, where the coherence pattern prohibits the diffusive spreading of correlations over the entire system and thus exhibits robust initial state fidelity (and purity of the densities). Note that here the constraint on Hilbert space, which results in a failure of global thermalization and the initial fidelity, should be of the same type of the repeated local measurement (on an individual bond or qubit), and the constraint on Hilbert space as well as the reduction on entanglement depends on the frequency of local projective measurement. The complexity of coherence field is enhanced with the raising frequency of local measurement, and the global thermalization (with saturated entanglement growth following area law) cannot be achieved until at the maximal frequency which involves the off-diagonal densities such that the system turns to, again, a local tensor product structure. Thus unlike the above *sq*-case, the coherence field (local oscillation) in *mm*-case generates the infinite number of bound states (quasiparticles) that allows the ballistical transport at finite energy. But the merged Loschmidt echo indicating the zero-energy limit with saturating scaling instead of

ballistical one. In fact, the static entanglement entropy (like the Renyi entropy) only depends on the variance of boundaries of Loschmidt echo, such that each subspace of *mm*-case has zero entropy which behave exactly like a pure state, and for arbitrary subsystems, the Renyi entropy (up to arbitrary order) of *sq*-case is always higher than that of *mm*-case if we do not consider the dynamics of entanglement (i.e., without considering the increasing complexity during unitary evolution).

In the *mm*-case, a large amount of bound states (mode) emerge discretely as can be seen from the Loschmidt echo, where the superpositional coherence is allowed between the open subsystems. Also, the discretely emergent non-Hermitian skin effect with unthermalized-type disentangling causes the absence of measurement-induced entanglement transition (volume-law to area-law)[28]. The weak disorder and the non-Hermiticity result in the delocalization in *mm*-case, which means the system is free from the constraints of integrability and many-body localization, and, in the mean time, without thermalization and global quantum correlation or entanglement[15].

Arbitrary densities  $\rho_{mm;\{i\}}$  therein (with  $\text{Num}\{i\} > 1$  and thus be the mixed state) behave as an ensemble of pure states[31], which act as an open subsystem interacting with infinite reservoirs[31], and thus the coherence plays the dominating role (with the off-diagonal part lacking large fluctuation). The skin effect is available for arbitrary strength of non-Hermiticity, thus it produces the disentangling (suppresses the entanglement and thermalization) in a different way compared to the measurement: The non-Hermiticity is realized by the constriction to a subspace in finite size (symmetry sector) with the conditioned (postselected) dynamic of quantum trajectories on the measurement outcomes, where exponentially many measurements are required. The measurements on the conditioned dynamics in non-Hermitian system return null results due to the lacking of average over trajectory ensemble as well as the absence of randomness in the measured dynamics.

In the presence of finite dissipation, while the non-Hermiticity refers to the microscopical continuous measurements with the conditioned evolution without quantum jump, there are discontinuous conditioned evolution with quantum jumps for the whole picture of *mm*-case. Those involved quantum jumps can be directly evidenced by the repeatedly merged Loschmidt echo, which also refers to the coherent field (local oscillator) in a system like optical cavity. *sq*-case always processes a linearly-in-time (volume law) to saturating (area law) transition, *mm*-case (without postselection) processes a volume-law entanglement without saturating[135] and exhibits persistent fluctuations with the increasing complexity of coherence configuration, i.e., the set of local Hamiltonian (disorder-free). It is such locality and coherence that guarantee the fidelity (as well as the subsystem purity).

### C. Realizations under measurement

The above-mentioned dissipation with measurements, which allows measurement-induced entanglement transition as well as other continuous phase transitions, always prompts the decoherence due to the raised system-bath coupling in frequency, consistent with the behavior of a Markovian open quantum system. In other words, there is a single local operator projected into the whole system which is Gaussian localized (ergodic and has extensive entropy). For a Gaussian distribution implied by the central limit theorem, the randomness and mutual independence is hypothesis[59] instead of a rigorously proven fact. One reason is the exponentially localized perturbations from local measurement will not affect the global locality and thermalization. This should be distinguished from the nonreciprocal dissipation (the origin of skin effect), which gives rise to discontinuous phase transition.

The magnitude of imaginary eigenenergies directly determines the instability of the delocalized phase against the absorption or emission of modes (quantum jump)[13]. Larger the imaginary part, smaller the uniform damping[138]. This is also in agreement with the no-jump condition for non-Hermitian dynamic in continuously measured quantum system, and thus effectively suppresses the entanglement through the local measurement. Further, the weak and frequent (strong and sparse) measurement results in the long-lived pure state (mixed state) with suppressed (enhanced) entanglement following the area-law (volume law). The former under weak measurement (Markovian process) occurs with broken parity-time ( $\mathcal{PT}$ ) symmetry [60, 61]; While the latter under strong measurement requires certain symmetries, like the time reversal symmetry[13], which is also consistent with the suppressed imaginary part of eigenenergies by localization (on-site disorder). The strong measurement usually refers to the projective one, during which the process of the system-probe coupling is much stronger than the energy scale of system, and consequently a weighted trajectory process volume-law (steady-state) entanglement. For the former case with weak measurement, the global localization caused by the dense measurement is the so-called quantum Zeno effect[66, 108, 112, 136, 138]. The Zeno effect, unique to the *sq*-case, is accompanied by the continuous measurements and continuous strong dissipations which suppress the fluctuation as well as heating up of the system[63, 112, 134, 135, 148] as a property unique to the nonequilibrium engineered dynamics, and thus protecting the topological order therein[81, 113], and the average over environmental non-Markovian noise realizations cause the non-Gaussian correlation under nonper-



turbative treatment. Note that here the disentangling (area law) due to the Zeno effect is distinct from that due to the projective measurements in *mm*-case, as the former stabilizes the measurement-induced phase transition while the latter hinder it. Here the suppression on fluctuation implies the common effect between the continuous strong dissipations and the on-site disorder which is capable to leads to localization even in non-Hermitian many-body system[40]. The diffusion-induced continuous dissipations here is nonlocal and related to the widely spreading quantum correlations. Another property similar to the Zeno effect is the nonstabilizerness whose additivity guarantees its global nature and can even be produced by a unitary operator by averaging over the ensemble of pure state trajectories of a full unitary group[110, 111]. The Zeno effect is most significant in the later stage of *sq*-case, whereas in early stage the large system size can enhance the robustness of entanglement grow against the classical stochastic dynamics by the quantum jumps[136, 153], i.e., lower the effect of dissipation. Note that the heating loss (suppression on entanglement production) here is different to that in the *mm*-case, but relies on the robust initial state property with non-Hermitian collapses and revivals[139], similar to the quantum cooling protocol of Ref.[146] which is by reducing the excited states back to ground states. While the Loschmidt echo directly indicates that the discrete symmetries only exists in *mm*-case with the jump-induced local dissipations (accompanied by the local dephasing and oscillatory behavior[112]) and dissipative coupling via the ballistic transports and synchronization, which is unique to a many-body system and representing the robust initial-state fidelity under the measurements at a finite rate[66, 88, 109, 151]. Except the many-body nature, the infinitely long time needed to loss the initial-state information also consistent with the thermodynamic limit in *mm*-case, where there are thermal baths holding well-defined temperature.

The entanglement transition arises from the sparse-to-dense measurement is invisible in the presence of skin effect or density-bath coupling through the measurements which results in trajectory-averaged evolution. In other word, it requires some temporal randomness[60, 65] to realize measurement-induced entanglement transition, e.g., in ergodic and nonintegrable system. Such randomness can be caused by the interacting effect (such that the free fermions system under weak measurement does not follows volume-law scaling[28, 136]), including the spin-orbit coupling between the up-spin fermions and down-spin fermions[61]. Here, the average over (trace over) trajectories (measurement outcomes) results in the dynamics of mixed state density matrix described by Lindblad master equation. Such statistic mixture necessarily produce area law short-range entanglement in the open boundary system, and allows: 1) The temporal randomness in dynamics or measurement outcomes under weak measurement, which is important in keeping mixed state and developing volume-law entanglement; 2) Unitary evolution; 3) Applications of the quantum channel[60, 77, 78, 81]. Despite the quantum information can be well preserved by a local quantum channel through coherent measurement[77], or by the exceptional points (defective degeneracies), there are nonlocal quantum channels in terms of ensemble average where the combined effect of non-Hermiticity and many-body property cause the weak postselection (where the nonlocality dominates and preclude the exceptional points), and the Lindblad master equation is the continuous limit of such a quantum channel[60, 75]. Note that such weak postselection case with significant randomness corresponds to the *mm*-case.

Distinct from the measurement-induced phase transitions deeply affect by the disorder in open quantum system coupled to a Markovian environment (i.e., the process of repeated weak nonlocal measurements)[13, 60, 61], the skin effect does not affected by the disorders. Importantly, in the presence of unitary conditional feedback together with the projective measurement, the system no necessarily prohibit the measurement-induced entanglement transition[62, 63], this generally corresponds to the case of weak measurement. Consistent with our above analysis, such weak measurement scheme, which is free from the skin effect as well as the induced disentangling, corresponds to the *sq*-case: The quantum state diffuse over the whole system and evolve coherently (Heisenberg evolution) under measurement,  $|\psi\rangle \rightarrow e^{-iH\Delta t}|\psi\rangle$  with the time step  $\Delta t$  (strength of system-probe coupling) be comparable with the time-scale (energy-scale) of the system. Consistent with the behaviors unique to the *sq*-case, the system and the measuring setups are collectively in a pure state (closed) while the system by itself is in a mixed state[60, 61]. Here the coherent evolution should be distinguished from the coherences in the *mm*-case which relies on skin effect and individual quantum trajectory. In *mm*-case the system by itself relax to a pure state in terms of coherence pattern,

As detailed in the discussion on *mm*-case, we consider the short-range entanglement as the main source of volume-law scaling before the thermalization (Hermitian limit). Refs[66–69, 71] also suggest that the entanglement is suppressed by measurements upto a certain frequency for finite probability of measurement outcome. The projective local measurement[28, 34, 39, 91] projects the cavity mode into photon-number eigenstates, with the resulting photon number operator be Hermitian and commutes with the Hamiltonian (which governs the unitary evolution of the stochastic states). Except the measurement outcomes, the stochasticity could originates from the random space-time sites of noises (i.e., the quenched disorder which will leads to localization and entanglement suppression), and such stochasticity disappears for Poissonian measurement which take place randomly at each space-time site regardless of the specific probability[66]. While when the probability takes effect, the space-time

sites in unitary circuit are biased by the nongeneralized measurements, where both the measurements on sites (through gates) and the measurement outcomes are specified (e.g., by postselection), and results in nonunitary dynamics[60, 66]. This is exactly the *sq*-case, which corresponds to a generic (nonintegrable) system lacking the noisy and subject to global thermalization with continuous measurements.

Importantly, we stress that the full dynamics of *sq* (*mm*)-case is nonunitary (unitary) in perspective of the trajectories and the entanglement growth, corresponding to the open system coupled to the nonthermal (thermal) non-Markovian (Markovian) environment with continuous (discontinuous) measurements, diffusion-(jumps)-induced nonlocal (local) dissipations, and weak (strong) system-bath coupling due to the incomparable (comparable) timescales, as described by the single-particle (many-body) picture. In other word, for *sq*-case (*mm*-case) under weak (strong) measurement which disallows (allows) the decoupling of sectors, there is the finite (infinite) temperature average or non-Gaussian (Gaussian) correlation that is nonlinear (linear) on state through definite (indefinite) heating up during evolution, together with an ill-defined (well-defined) bath temperature for the nonintegrable (integrable) many-body system which leads to ergodicity or generic feature (nonergodicity or nongeneric feature) and the thermalization happened at a single trajectory level (trajectory ensemble level). It is also more easy to realize thermal equilibrium (nonequilibrium) in *mm*-(*sq*)-case as evidenced by the short-range order (long-range order) and unitary (nonunitary) dynamics therein[132, 136, 141, 153].

In perspective of the generalized Gibbs ensemble and weak ETH in thermodynamic limit (due to the small fraction of unbiased and unpostselected nonthermal states), for *mm*-case, the countable quantum jumps can be treated as the weak perturbations for the breaking of integrability, localizations, and quantum coherence. In disordered phase of the *mm*-case, there are extensive localization length with large dissipation rate (thus, projective measurement in high frequency) and short-range hopping (thus, short-range entanglement). In *mm*-case, the strong Markovian (white) noise from environment will enlarge the time of relaxation toward the (unitary) Hermitian limit, exceeds the waiting time between quantum jumps, such that the averaging over noise trajectories allows the mapping onto Lindblad master equation where the jump operators appear in the incoherence (dissipative) part. It is such long timescale that bound the volume-law (ballistic) growth of entanglement. Such perturbation is too weak to causes thermalization and meanwhile the perturbation theory is validate by the significant (nonuniform) gaps between eigenvalues in this case (i.e., discrete levels due to the discontinuous jumps). Despite the short-range entanglement is suppressed by the skin effect and noise which has the same effect with perturbations (jumps), the deterministic Heisenberg coupling and the kinetical constraints on Hilbert space due to the coherences results in local operators and the ballistic entanglement growth (as a result of interaction effect). Consistent with our finding, the diffusive fast relaxation is possible even in *mm*-case in strong-noise limit under weak-perturbative treatment[96, 97, 99–101], despite the diffusion here is suppressed by the skin effect. Note that the diffusion constant is inversely proportional to the relaxation timescale, noise amplitude (noise strength) or measurement (dissipation) rate, and disorder strength in strong (Markovian) noise case and weak (non-Markovian) noise case, respectively, where the squared disorder strength can be estimated as the second moment of noise in the latter case[96, 100, 103, 120].

While the integrability is completely broken by the infinite photon flux in *sq* case, where the weak but frequently repeated measurement (also known as generalized or non-projective measurement), each as well as every qubit (uncountable infinite photon flux) being measured at each time step no matter how small the time step is, and allowing the entanglement transition[66, 70, 80]. Also, the Poissonian number statistics of the coherent local oscillator with infinitely large amplitude representing the photodetection or quantum jump counting is very large, such that it can be approximately as Gaussian (robust to interactions), by treating the field as a whole object and validating diverging two-point (auto)correlation function[43, 112, 136, 139], with local real-valued Gaussian noise (Wiener) increment and emergent quantum noise from the stochastic noise.

Thus there could be transitions between nonunitary and unitary dynamics: As mentioned in Sec.IV A, a nonunitary dynamics with nonuniform continuous measurement can be guaranteed by a relaxation time shorter than that the waiting time between quantum jumps (or projective measurements)[80, 90], and the absence of interaction effect therein allows the measurement-induced phase transition as well as the criticality phenomenon[90, 118]. The high measurement rate (frequency) cause a short Zeno timescale and coarse-grained dynamics due to the incomparable timescales between system and bath [63, 80, 90, 96, 117, 121, 137, 144]. The fast relaxation to equilibrium corresponds to the small dissipation rate  $\gamma_i$ , low occupation fraction, and small noise (two-point) correlation in non-Markovian limit[96] which consistent with the weak noise limit and the Lindblad master equation dominated by the unperturbed (dissipative and uncoherented) part. Fast relaxation gives rise to the dynamical stability due to the suppressed imaginary part of effective non-Hermitian Hamiltonian, as well as the transition to localized phase at steady state in the long-time limit with uniform projective measurement (and thus becomes less sensitive to the measurement unlike the conditioned or postselected dynamics), where the equilibrium state (ensemble average of trajectories[90] or coherent superpositions of symmetry-breaking states[94]), becomes indistinguishable

from the time averaged state[80, 93]. Thus, in conclusion, the *sq*-case involving two stages in evolution: In early stage there are weak but frequent measurements (continuously) and strong system-probe coupling[80], dominated by nonunitary (non-Hermitian) stochastic dynamics and algebraic decaying with gapless nature toward the pure state. In late stage where the system approaches the equilibrium steady state, it becomes more significant for the nonextensive character of the localization length and density imbalance of particle distribution due to the vanishingly small dissipation rate and system-probe coupling, in which case the (group) velocity is well-defined according to the long-range power-law hopping of free fermions[56] due to the absence of many-body feature, and meanwhile it is possible to realize unitary and Hermitian dynamics due to the emergent topological invariants[95] (e.g., the nontrivial  $\mathbb{Z}$  class[107]) which suppress the short-range entanglement and thus promote the transition from condensed phase (topologically trivial phase) to the topologically ordered pure state (the product state representing an ensemble). In the case of strong Markovian noise, even the shortest-range (nearest neighbor) incoherent hopping in perturbative treatment would lead to diffusion[120]. Note that, different to the "Hermiticity" of *mm*-case where there is power law decay (also including the Gaussian decay of decoherence by the strong system-bath coupling[115]), the "Hermiticity" in late-stage of *sq* case exhibits exponential decay where the locality is guaranteed by the large dissipative gap under nonunitary (disentangling) measurements[63, 104, 133], and this corresponds to the macroscopic response to the quantum jumps measured in a timescale (waiting time) larger than the fluctuation (scattering induced by imaginary potential[122]) timescale. Equivalently, the fast relaxation to the (pure) dark state in *sq*-case contributes to the global area law phase (e.g., the  $Z_2$ -type localized phase)[15, 63]. The condensed phase here in *mm*-case does not involve the fluctuation and dissipation stochastic contributions from the quantum jumps, and the power-law decay guarantee the (solvable) nonperturbative characteristic[104, 116, 117, 127] (until the sparse measurements and dissipations as well as perturbative contribution from jumps set in). Despite as a hallmark of valid bosonization and condensation and kinetic constraint in Hilbert space[51, 104, 127], the diffusive power-law scaling of long-range hopping and fluctuations is available in *sq*-case (attributed to the ergodicity and weak measurements) [39, 56, 96, 126, 128–130], e.g., the system with anisotropic power-law long-range dipolar interactions[132, 134, 142, 153] which contributes to the polarization and conservation of collective spin and critically slow thermalization (e.g., slow relaxation of magnetization or spin polarization)[142, 145, 153] in contrast to the fast Markovian dephasing (e.g., the global depolarizing noise channel[174, 175]).

Distinct from our above statement in many-body perspective that the *mm*-case is dominated by algebraic decay with power-law short-range correlations (due to the skin effect induced, e.g., by the sparse measurements) and the depinning of particle density caused by unitary dynamics (delocalized phase[15]), each single-particle Gaussian state in *mm*-case exhibits exponentially decaying short-range correlation (with area law entanglement) in the case of logarithmically growing (unbound) correlation length[63], e.g., in massive boson mode, but such area law phase induced by exponentially decaying correlations (together with the macroscopic wave function for photons or condensed bosons, i.e., paired fermions with short-range hopping) only takes a little fraction in the *mm*-case due to the isotropic nature and the encoded robust initial state information as long as the system is dominated by the condensation. This is also in agreement with [136], where the classical stochastic dynamics can be overwhelmed from the many-body microscopic details. Despite the skin effect, *mm*-case is dominated by the algebra (power-law) decaying, and indefinitely heating up toward the infinite temperature and maximally mixed steady state, as can be evidenced by the absence of a characteristic time scale in the long-time dynamics and the presence of significant phase fluctuation (suppressed by the sparse measurements and implies no thermalization[134–137]; see Fig.2) and gapless structure of Hermitian measurement operator or Liouville superoperator[133]. Thus, the entanglement entropy loss (heat loss) induced by the sparse quantum jumps is overwhelmed by the entanglement entropy gain due to the non-Hermitian evolution in each sector as well as the non-Gaussian interactions[134, 136].

Thus in perspective of the whole system, the topological order pure state with long-range entanglement and lower measurement rate is favored in *sq*-case where particle-hole symmetry is broken (irreversible) by the long-range hopping, while disordered phase in constricted Hilberts space with short-range entanglement and higher measurement rate is favored in *mm*-case where particle-hole symmetry is preserved (reversible) by the short-range hopping[104, 106, 107, 122]. The topological nontrivial phase in *sq*-case, as stabilized by engineered dissipations, refers to the global symmetries, like the  $\mathbb{Z}$  class, to guarantees the bulk-boundary correspondence or the valid description of winding number; While the topological trivial phase refers to the discrete symmetrie, like the particle-hole symmetry. Such disordered-to-ordered transition is also reminiscent of the strong-to-weak spontaneous symmetry breaking (in opposite to the effect of local decoherence from a short-depth local quantum channel[44, 78, 81, 113, 114, 117, 153]), or the reversible-to-irreversible transition, where a description of bosonization is valid in Hermitian limit (*mm*) as evidenced by the linear infinite temperature average (Gaussian correlation) as well as the unsuppressed heating up and noise-induced fluctuations[63, 104, 112, 116, 121], but breaks down in low-density regime with nonunitary dynamics and nonperturbative treatment under continuous post-selected

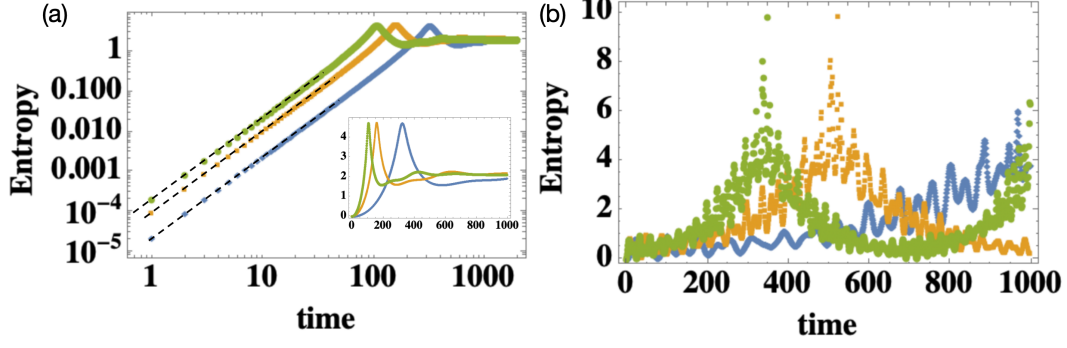


Figure 1. Von Neumann entropy  $-\ln \text{Tr} D^2$  for *sq* (left) and *mm* (right) cases, which can be termed as microscopically defined entropy and thermodynamic entropy, respectively. Blue, orange to green dots represent the increasing system size at balanced partitions. The transition of linear (volume law) scaling to saturation toward a system-size-independent value (area law) can be seen in *sq*-case. The linear growth of entropy in early time is consistent with the scrambling (spreading of local information) with constant slope described by classical Lyapunov exponent[160], Thus for different system size, there are different scrambling time but same Lyapunov exponent. while the quantum mechanics with interacting effect only sets in latter as exhibited by the power-law growth toward the maximal entropy which corresponds to the dip in purity (see Fig.7). Note that the maximal entropy here does not corresponds to the maximal mixture as shown in Fig.7. The entropy in *mm*-case is dominated by the quantum mechanics. The revival behavior in *mm*-case results in a periodically fluctuating entropy, which should be distinguished from the macroscopic mechanical oscillations[180] and can be fitted by the conformal field theory (discontinuous) in the analysis of finite size scaling[39, 149, 166]. We also verify that the entropy here equals to the negative of the logarithmic negativity  $-\ln(\text{Tr} D^{1/2})^2$ [155]. The scheme (a) automatically arrives the balanced partition due to the densest measurement; While the scheme (b) admits arbitrary partitions as revealed by the entanglement between the unitarily or nonunitarily evolved pure state  $|\rho_0\rangle\langle\rho_0|$  and the rest. For (a), it is reasonable to suspect that, the peak of entropy between the (sub)volume phase in early time and area law phase in late time, which sharpens with increasing size, will vanish in the large system size limit, and the scrambling will also vanish.

measurements[63, 104]. The Anderson localization is favored under stronger (static) disorder in the late-time stage with saturated localization length. Thus the *sq*-case with Wiener process (Brownian motion)[90, 97, 98] involving both the deterministic (single trajectory level) and Ito stochastic under weak (dephasing) noise. While a unitary dynamics emerges when the uniformly measurement is performed to ensure constant dissipation rate  $\gamma_i$ , and  $\sum_i L_i^\dagger L_i$  is bounded to be a conserved quantity which is inversely proportional to the waiting time between projective measurements[90].

For weighted trajectories in *mm* case, the unitary evolution guarantees the open boundary condition, and the well preserved initial quantum information due to the interacting effect (in a non-Hermitian way) is consistent with the periodic drive which is widely seen in realizing the unitary model, as a example, the ensemble randomness of unitary gates in a unitary circuit induced the chaos (short-range entanglement). Thus the local unitary gates equivalents to the effect of nonlocal measurement, reminiscent of the forward scattering of thermal eigenstates. In classical configuration, the randomness in locations of projective measurement is necessary to observe volume-law to area-law phase transition through the zeroth Rényi entropy  $S_0 = \ln \text{Rank}(\rho)$ , which is sensitive to the jump-induced weak perturbation due to the rank-dependence[83] and has less contribution to the entropy[66]. where the ratio  $S_0/\ln t$  exhibits scale invariance at critical measurement rate with the logarithmic long-range entanglement[44, 83, 84] This is consistent with the classical analogy of the measurement-induced entanglement phase transition, like the local-projection-induced information freezing[86], or the driven-induced synchronization[85, 109].

## V. METHOD AND NUMERICS

We define the densities of the two classes as  $\rho_{mm} := \sum_i |\psi_i\rangle\langle\psi_i|$ ,  $\rho_{sq} := \sum_i |\psi_i\rangle\langle\psi_i^*|$ . For  $\rho_{sq}$  such asymmetry construction (off-diagonal) of the density is also consistent with that in the content of Dicke states[169, 171]. The reduced form can be seen by the state of the combined system environment  $|\rho_{SE}\rangle = \sum_i |\psi_i\rangle|\mathcal{E}_i\rangle$  with  $\langle\mathcal{E}_i|\mathcal{E}_j\rangle = \langle\mathcal{E}_i|\mathcal{E}_j^*\rangle = \delta_{ij}$ . The complex eigenstates are prepared aimed to obtaining the non-Hermitian operator  $\Psi$  whose elements follow the distribution of Gaussian ensemble, upto second and fourth moments, and reads, when consider two real eigenvalues,  $\Psi = \lambda_\alpha \Psi_\alpha + \lambda_\beta \Psi_\beta$  For a general route of construction, see Refs.[8, 150]. The densities

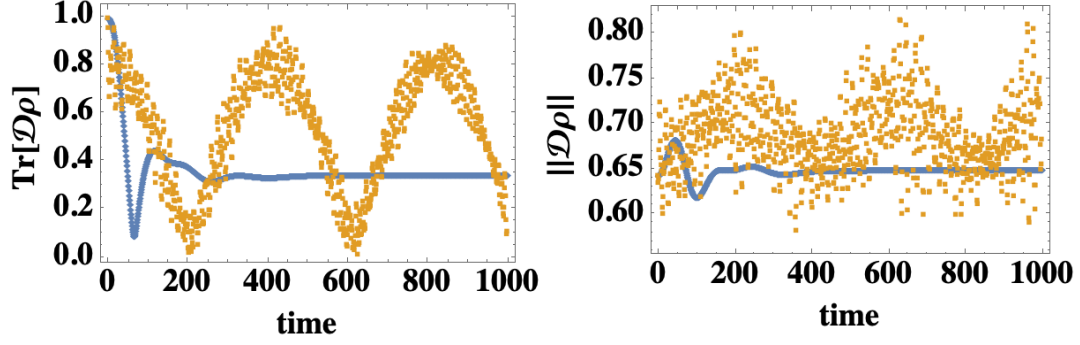


Figure 2. Evolutions of trace and norm of the dissipative term for *sq* (blue) and *mm* (orange) cases.. The exponential decay and incoherence feature can be seen from the *sq*-case, reflecting that the dissipative terms are nondegenerated or nondefectively degenerated. While the algebraic decay is hard to recognize from the *mm*-case, due to the complicated coherence (averaged) pattern. The left panel is indeed a conditioned expectation of the stochastic object which does not depend on Wiener increment (Markovian noise) but on stochastic increments at earlier times[119].

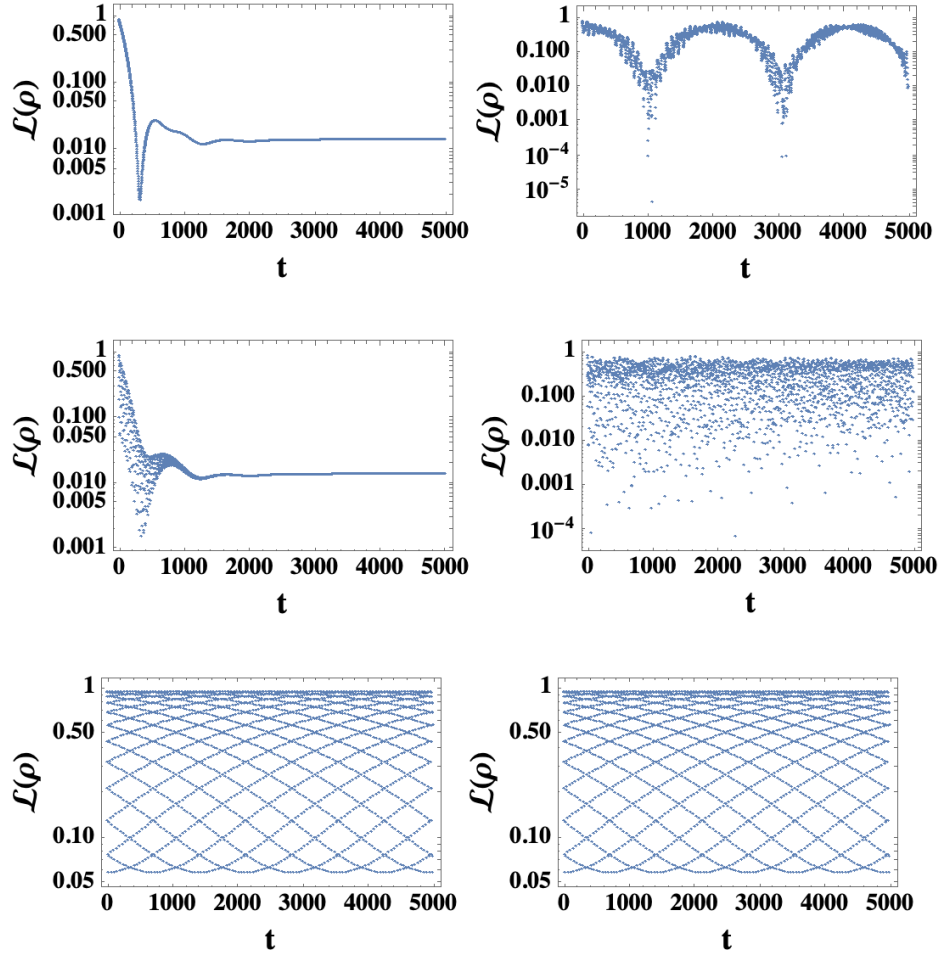


Figure 3. Loschmidt echo for *sq* (left) and *mm* (right) cases. First, second, and last rows correspond to the full, nondegenerated, and degenerated (NDD) eigenspaces, respectively.



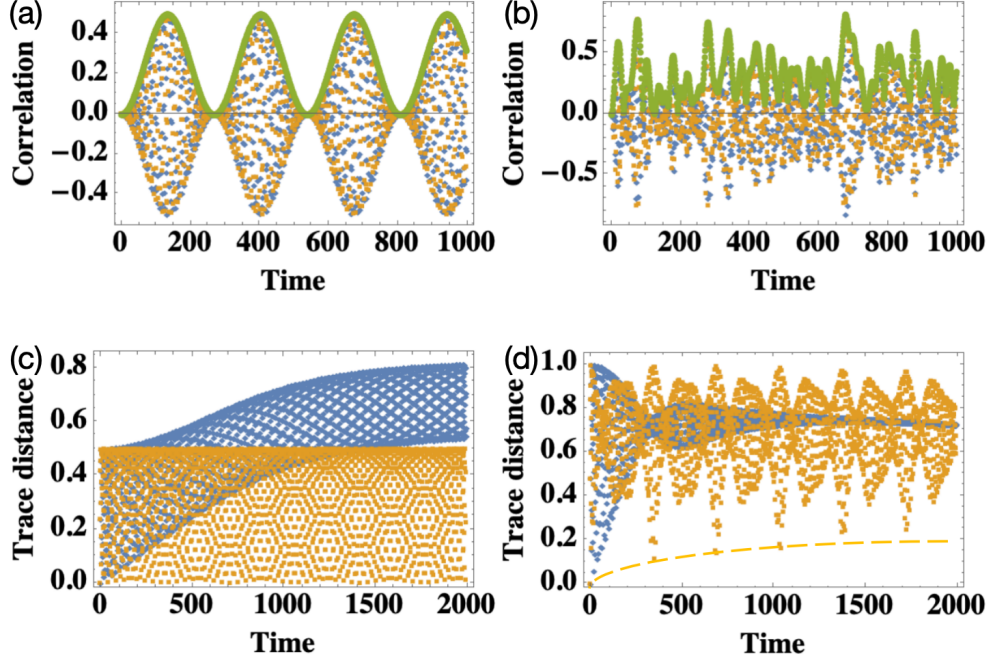


Figure 4. (a) and (b) show the  $e^{i(\rho_i+\rho_j)t} - e^{i\rho_i t}e^{i\rho_j t}$  ( $\neq 0$  only for  $\rho^\dagger = \rho$ ) representing the periodically oscillating classical correlations (or noncommutativity) between the two arbitrary states of the  $mm$ -case, for incomplete and complete basis, respectively. Such pairwise correlations is unique to the  $mm$ -case, due to the lacking of macroscopic oscillation[180]. Blue, orange, and green dots represent the real, imaginary, and absolute parts. Such correlations, which exist between arbitrarily two components in the  $mm$ -case, cause the delocalization and the weakened boundary driving effect. This also make the construction of Floquet driving potential available, and such correlation (in contrast to the entanglement) can also be reflected by the separability across all bipartitions[180, 182], which is realized by the projective measurements on one subsystem and cause the statistical mixture of pure states (chaotic projected ensemble) in the another subsystem (disentangling)[181]. Coherences are allowed between these mixed subsystems. (c) and (d) show the trace distance  $\frac{1}{2}\|D_i - D_j\|$  ( $\|\cdot\|$  representing the trace norm), which witness the distinguishability between states  $D_i$  and  $D_j$  (initially pure states), for incomplete and complete basis, respectively, with blue and orange dots correspond to the  $sq$ -case (blue) and  $mm$ -case (orange), respectively. For complete basis, a uncontinuously reduction of trace distance for  $sq$ -case reveals that the existence of non-Markovian process in early stage. Despite not being shown here, we have verified that, the Jensen-Shannon divergence[179] of  $sq$ -case reduces to zero at long-time. Still, the non-Markovianity in  $mm$ -case, as revealed by the memory effect and environment-to-system information backflow, causes the nonmonotonic behavior of trace distance as well as the distinguishability between the two quantum states, and a seperable mode into the hot and cool ones. Similar nonmonotonic behavior in entanglement and decoherence function are studied in Refs.[178, 183]. The trace distance in (d) for  $mm$ -case exhibits persistent temporal fluctuations despite more and more homogeneous compares to initial as indicated by the dashed line. It is the correlations cause the revival of trace distance and environment-to-system backflow of information. Ref.[173] indicates a possible realization of such a scenario by the balanced interplay between interaction (with bath) and tunneling.

$D_{mm/sq}(t) = e^{i\rho_{mm/sq}t}(\sum_i |\psi_i\rangle)(\sum_i \langle\psi_i|)$ , whose square of trace is the Loschmidt echo, is important in revealing the difference between  $sq$  and  $mm$  cases. The initial state for both cases are pure state and unentangled. Available convex sum form for densities in  $mm$ -case (diagonal in the Schmidt basis[156]) agrees with the absence of topological order therein. Environmental decoherence effect (off-diagonal fluctuation) emerges when  $\langle\mathcal{E}_i|\mathcal{E}_j\rangle \neq 0$  for  $i \neq j$ , and this will suppress the entanglement and cause the gapless structure for  $mm$ -case and early stage of  $sq$ -case. Such decoherence and off-diagonal fluctuation will be suppressed by larger system size in  $sq$ -case, and decay with time toward the gapped (area law). Also, the entropy for product state  $(\sum_i |\psi_i\rangle)(\sum_i \langle\psi_i^*|)$  converges to  $1/2^N \approx 0.0039$  (maximally mixed density) where  $N = 8$  here is the maximal number of independent states, which indicating the possible relation to the Page value[161]. Also, as shown in Fig.4, the correlation dynamics revealed by the expectation of covariance matrix (nonlocal density; fermion Green's function)[129, 164, 170]  $\text{Tr}[D_{mm/sq}(t)]$ , reflects that in  $sq$ -case a trajectory in a  $2^N$ -dimensional space can be encoded into the evolution of the  $N \times N$  observable  $e^{-i\rho_{mm/sq}t}$ , where  $\overline{\rho_{sq/mm}} = \overline{e^{-i\rho_{sq/mm}t}}_{t=0} = \lim_{t \rightarrow \infty} |\text{Tr}[\frac{e^{-i\rho_{sq}t}}{N||e^{-i\rho_{sq}t}}]| = (\lim_{t \rightarrow \infty} |\text{Tr}[\frac{D_{sq}(t)}{||D_{sq}(t)||}])|^2 = \frac{1}{N}$ . A polynomial complexity in system size is only available in the late-stage of  $sq$ -case, where the simplification is available due to

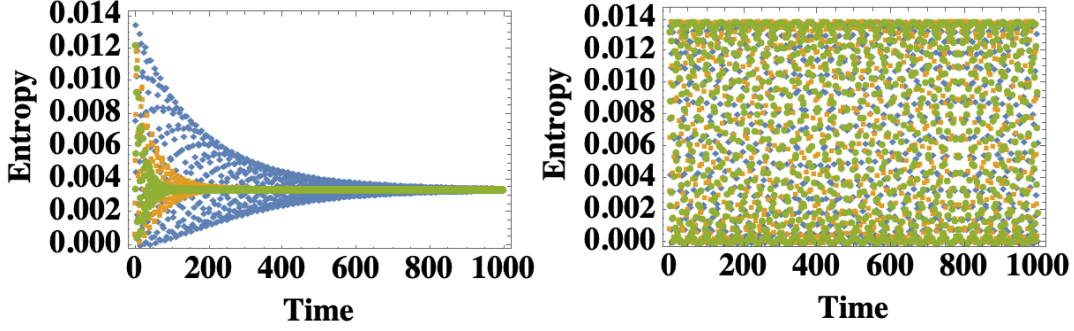


Figure 5. Von Neumann entropy for product states  $(\sum_i |\psi_i\rangle)(\sum_i \langle\psi_i^*|)$  (*sq*) and  $(\sum_i |\psi_i\rangle)(\sum_i \langle\psi_i|)$  (*mm*). The fixed bulk pattern here indicates the possibility to be free from thermalization, which disappears in *sq*-case with the nonunitary evolution which varies the upper and lower boundaries. Similar to Fig.1(a), a gapless (volume law with density depinning) to gapped (area law with density pinning) transition can be seen for *sq*-case (i.e., nonequilibrium boundary to equilibrium boundary crossover[157] with exponentially slow disentangling consisting with Lorentzian distribution). For product state in *mm*-case, even the local thermalization (induced by the coupling to degrees of freedom of bath) cannot be seen. The fully engineered entropy evolution in long-time (by the dissipative environment) in *sq*-case reflects the difference between the few-body cluster entanglement and the many-body (fluctuating) one.

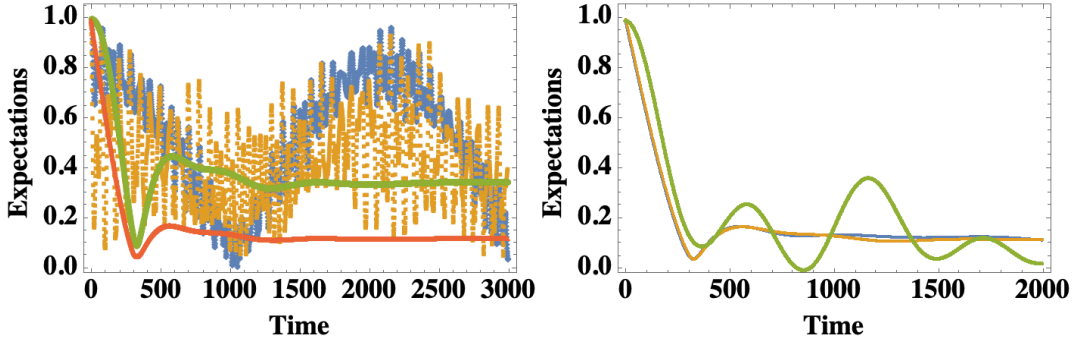


Figure 6. (Left)  $|\text{Tr}[\frac{D_{mm}(t)}{\|D_{mm}(t)\|}]|$  (blue),  $|\text{Tr}[\frac{e^{-i\rho_{mm}t}}{N\|e^{-i\rho_{mm}t}\|}]|$  (orange),  $|\text{Tr}[\frac{D_{sq}(t)}{\|D_{sq}(t)\|}]|$  (green), and  $|\text{Tr}[\frac{e^{-i\rho_{sq}t}}{N\|e^{-i\rho_{sq}t}\|}]|$  (carmine). The last two approach to  $\sqrt{\frac{1}{N}}$  and  $\frac{1}{N}$ , respectively, in long-time. The variance of non-Hermitia observable[180] as well as the Jensen-Shannon divergence (JSD) also support the conclusion that the *mm*-case has much robust uncertainty compares to the *sq*-case. Note that here the uncertainty and randomness are not due to the selections by measurement apparatus, which mean the Green function here does not contains a self-energy term. (Right) The expectation  $|\text{Tr}[\frac{D_{sq}(t)}{\|D_{sq}(t)\|}]| = \langle\rho_0|e^{i\rho_{sq}t}|\rho_0\rangle$  (Orange; without consider the perturbation from measurement apparatus) and  $\langle\rho'_0|e^{i\rho_{sq}t}|\rho'_0\rangle$  (Blue; consider the perturbation from measurement apparatus). The effect measurement apparatus here is small but finite due to the nonunitarity of  $e^{i\rho_{sq}t}$ . The traditional mass perturbation theory is invalid here. The postselection probability after measurement  $|\langle\rho'_0|\rho_0\rangle|^2$  (in the absence of interaction) is shown in color green. While in *mm*-case, the projective measurement suppress the long-range entanglement but does not cause the selections on measured states due to the effect of unique Markovian bath. Another reason is that we choose a time-independent basis  $\langle\rho_0|\rho_0\rangle$ . Consequently, the mapping  $|\rho_0\rangle \rightarrow |\rho'_0\rangle$  does not cause any new conservations. This indeed reflects the existence of response to the global quench in *mm*-case, just like the complete thermal state in late stage of *sq*-case, i.e., the common characteristic between the Markovian system in *sq*-case and the unique Markovian bath in *mm*-case.

the absence of persistive fluctuates in Hilbert space[166] and the Lieb-Robinson bounds and nonunitary scrambling light cones. Also, the incoherent coupling to the environment is absent in the late-stage of *sq*-case which is in agree with Refs.[129, 164]. While such decoherence as well as stochastic dynamics is persistent in *mm*-case, due to the restricted Hilbert space and disorders which guarantee the accessibility of (maximally mixed) infinite-temperature featureless equilibrium state in long-time limit. Despite the classical stochastic processes, like the random diffusion, still observable in *mm*-case, the dynamics periodically back to the initial state, consistent with the microscopic theory. Such recurrence is recently studied in terms of the uncertainty relation[163, 165] and hybrid quantum circuit[166].

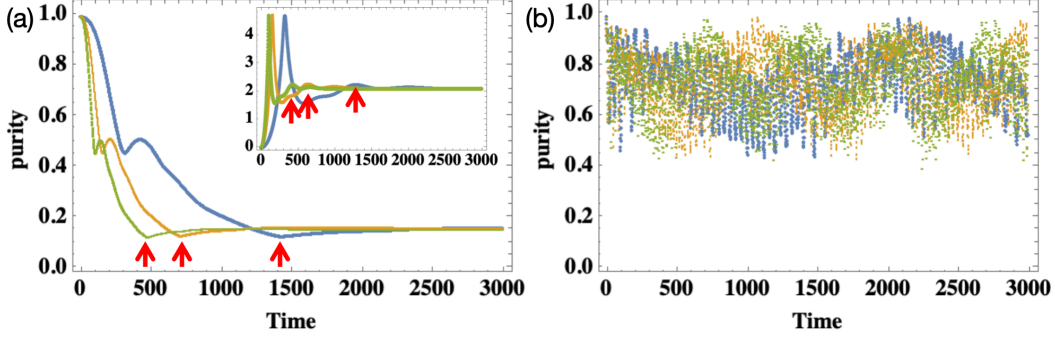


Figure 7. Purities  $\text{Tr}[D]^2$  for  $D = D_{sq}$  (a) and  $D = D_{mm}$  (b). Despite the global symmetry in *sq*-case, the purification back to the pure state is only available in the *mm*-case. This is because, in *sq*-case, the non-Markovian bath plays an essential role in engineering the dynamics of the system. The inset in (a) shows the entropy (the same with Fig.1(a)) for a comparison. There are two times of entanglement enhancement (purity decaying) in *sq*-case, which are due to the scrambling and the combination of monitoring and boundary-driven effect, respectively. The red arrows in (a) indicate the time when the long-range correlation as well as the area-law scaling become dominating (entanglement becomes nonextensive due to the absence of scrambling), implying the exponential decay and strong localization[159] such that the Gaussian (exponentiated bilinear) is achievable. In late-stage of *sq*-case (after the red arrows), the continuous monitoring from the dissipative environment cause the decay of entropy to the finite value.

As we shown in Fig.1(a), for *sq*-case, the entanglement entropy begin with a linear increase following the (sub)volume law, and then power law growth to maximal value. The enhancement of entanglement in this stage mainly originates from the increase of correlation range, during which process the non-Gaussian interactions be suppressed due to the global dephasing. The peak of entropy between the (sub)volume phase in early time and area law phase in late time, which sharpens with increasing size, is novel (robust against the variance of system size as opposite to the case in Ref.[168]), and corresponding to the beginning of a short purifying process as shown in Fig.7. After the maximal entropy, there is firstly a obvious power law decay (critical phase) and them a unobtrusive logarithmical increase, but the whole decay process toward the long-time (nonequilibrium) steady state can be enveloped by a exponentially fluctuating decay, as agreed by the emergent gapped mode and single-particle character. The entropy starts to decay when the entanglement production due to the elongated range of interactions cannot catch up with the annihilation due to the weakened interaction strength. In early stage of *sq*-case, which is gapless and system-size-dependent, the entanglement entropy deviates from the prediction of nonunitary conformal field theories and the central charge of the non-Hermitian system becomes invalid. The latter stage of *sq*-case has same similarities with the dynamical mean field theory, i.e., the suppressed entropy and fluctuations. But for DMFT, instead of the global symmetry, it is the local Markovian drive which causes the fast dephasing, and the non-Markovian bath algebraically decay with the increasing lattice connectivity (in a next-nearest interacting model)[148, 152]. Our result also shows that, larger system size (integer multiples of a complete basis to ensure the global dephasing) cause faster relaxation toward the nonequilibrium steady state at finite temperature, and also faster growth to the maximal entropy. This is because larger system size induces stronger suppression on the non-Gaussian interaction (and the associate averaging effect), which is the same with the effect of denser measurement[136]. The exponential decay in latter stage reflecting the area law region, is faster for smaller system size and thus larger gap of Liouville superoperator, in agree with Ref.[151]. Furthermore, there is a correlation length (or coherence length) effect which is unique to the non-Hermitian dynamics of *sq*-case as shown in Fig.1(a) and Fig.5(a), indicating the gapless-to-gapped transition (noiseless to noisy contribution) as well as the transition from Hermitian power-law decay to non-Hermitian exponential (faster) decay, which is indeed due to the Zeno effect[144]. Such gapless-to-gapped transition of the *sq*-case can be continuously turned by varying the strength of long-range correlation, which has a competition with the dense measurement. The emergent entropy saturation and the area-law scaling, i.e., (sub)system-size-independence, is actually due to the kick as indicated by the red arrows, which indicating the quantum critical behavior and whose appearing time is, however, (sub)system-size-dependent. The opening up of a gap trends to suppressing the imaginary part of the eigenvalues as well as the correlation propagation. Such transition only happen in large distance where there is scale invariant ground state (massless dark state[63]). The red arrow in Fig.1(a) indicate when the system approaching the area-law phase with the length-scale-dependent mass term, during which process the entanglement being destroyed by the quantum state diffusion, and the monitoring efficiency is improved[168] as verified by the increased weight of Gaussian  $\hat{I}$ to noise in the homodyne current which consist of the

fermion current[119] and Gaussian Itô noise. We also notice that, there are two times of entanglement enhancement (purity decaying) in *sq*-case which are due to the scrambling and the combination of monitoring and boundary-driven effect, respectively, and there is a cooling (purify) process that occurs intermittently whose behavior follows an algebraically fast relaxation which is different from the decay due to the diffusion limit (after the red arrow). In scrambling (early time) stage as shown in early time of Fig.1(a), as we increase the system size, the entropy increase but more and more slowly, which means it indeed follows subvolume scaling ( $\sim L^\nu$ ;  $0 < \nu < 1$ ) especially at large system size, consistent with the result of long-range entanglement[166]. Due to the densest measurement applied in *sq*-case, it is filling-, or partition- configuration-independent[39, 45, 128, 166], or we can treating it as arriving at the balanced partitions ( $N_\psi = N_\mathcal{E}$ ). like the case where  $N_\psi = N_\mathcal{E} \rightarrow \infty$  (fully symmetry-broken phase[23]; like the symmetry of superpositions[63, 133]). This is also consistent with the possible emergence of saturated entropy and vanishing gap with increasing system size even in early stage[144]. The partition- as well as system-size-independent noisy contribution emerges in the gapped phase (late stage of *sq*-case with overwhelming Gaussian disorder) or the gapless phase but with infinite system size (early stage of *sq*-case). The gapless-to-gapped transition can also be recognized as the delocalized-to-localized transition where the system-size-independent mixed state gives rise to the localization[166] as unique to the *sq*-case, where the entanglement enhancement is consistent with those found in few-body systems with long-range correlation, correlated dissipation and noise from non-Markovian bath[174]. Just like the (sub)volume law, the (sub)additivity of entanglement should be seen in the early stage of *sq*-case, signing the portion of integrability[88, 176]. The existence of gapless many-body spectrum in the early stage of *sq*-case also indicates the possible coexistence of disorder- and skin-effect-induced localizations in the bulk and boundary, respectively, as can be seen from the Loschmidt echo of the nondegenerated part (Fig.3) and numerically studied in Ref.[95]. While as the gap opens up, all states exponentially localized into the boundary and share the same local structure. It is also the lacking of integrability and all-to-all correlation (entanglement) in the later stage reduce the entropic uncertainty as well as the environment-to-system information backflow[177, 178]. Similar behaviors can be observed in Fig.6, We can see that the expectations are similar in the presence and absence of measurement basis, which implies the measurement apparatus plays little role here. In the other hand, of intermediate case (between *sq*- and *mm*-cases), the weak measurement on on-Hermitian observables are considered Ref.[184].

Consistent with the results in Ref.[184], here the non-Hermitian and unitary observables  $O_{nH} = e^{-i\rho_{mm}t}$  ( $t \neq 0$ ) is full-rank such that it can be decomposed into  $O_{nH} = U_{mm}R_{mm}$  with positive definite  $R_{mm} = \sqrt{O_{nH}^\dagger O_{nH}}$  and  $U_{mm} = \frac{O_{nH}}{\sqrt{O_{nH}^\dagger O_{nH}}}$  ( $U_{mm}^\dagger U_{mm} = I$ ). Then we can verify that  $\langle \rho_0 | O_{nH} | \rho_0 \rangle = \langle \rho'_0 | R_{mm} | \rho_0 \rangle = \langle \rho'_0 | O_{nH} | \rho'_0 \rangle$ , with  $|\rho'_0\rangle = U_{mm}^\dagger |\rho_0\rangle$  and  $\langle \rho'_0 | R_{mm} | \rho_0 \rangle / \langle \rho'_0 | \rho_0 \rangle = 1$ . The role of measurement apparatus can then be taken into account by preselecting the  $|\rho_0\rangle$ , or equivalently, postselecting the  $|\rho'_0\rangle$ , where the perturbations from measurement can be revealed by the nonzero imaginary part  $\text{Im}\langle \rho'_0 | R_{mm} | \rho_0 \rangle / \langle \rho'_0 | \rho_0 \rangle \neq 0$ . Thus the mapping  $|\rho_0\rangle \rightarrow |\rho'_0\rangle$  does not generates any new symmetries, instead, zero imaginary part of  $\langle \rho'_0 | R_{mm} | \rho_0 \rangle / \langle \rho'_0 | \rho_0 \rangle$ . guarantees the existence of response to the global quench in *mm*-case.

In the numerics as shown in Fig.2, we consider the case totally dominated by the dissipative process such that the unitary part (i.e., evolution and decoherence due to the system Hamiltonian) in Lindblad master equation is vanished. This cause the complete fail of perturbative treatment (e.g., the one introduced in Ref.[133] which is implemented by considering the steady state of nonperturbed part be a pure state).

An efficient way to enhance the noise from the environment's measurement is replacing the  $-\ln \text{Tr} D^2$  by  $-\ln \sum_i \text{Tr} \rho_i^2$  where  $\sum_i \rho_i = D$ , which cause a long-time steady state closer to a product state with much lower entanglement compares to Fig.1 and similar in mechanism to Fig.?? (by fill in the off-diagonal components such that it becomes fail to estimate the expectation value from local observable like the single-particle macroscopic sample). Obviously, this also corresponds to a purifying for *sq*-case.

For Loschmidt echo shown in Fig.3, we define the initial state  $|\rho_0\rangle = \sum_i |\psi_i\rangle$ , and estimate the overlap  $\mathcal{L}(\rho, \rho', \dots) := \frac{|\langle \rho_0 | e^{-i\rho t} e^{i\rho' t} \dots | \rho_0 \rangle|^2}{||e^{i\rho t} e^{-i\rho' t} \dots||^2}$ . Note that for *sq*-case, due to the nonunitarity, a artificial renormalization by the squared norm is necessary to avoid the diverging as we shown in Ref.[147]. In nondegenerated region, eigenstates in *sq*-case are mutually independent, while those in *mm*-case are mutually dependent. This can be easily verified by comparing  $\mathcal{L}(\rho + \rho', \dots)$  and  $\mathcal{L}(\rho, \rho', \dots)$ , e.g.,  $\frac{|\langle \rho_0 | e^{-i\rho_{mm}t} | \rho_0 \rangle|^2}{||e^{-i\rho_{mm}t}||^2}$  and  $\frac{|\langle \rho_0 | e^{-i\sum_{i=1}^j |\psi_i\rangle \langle \psi_i| t} e^{-i\sum_{i=j+1}^N |\psi_i\rangle \langle \psi_i| t} | \rho_0 \rangle|^2}{||e^{-i\sum_{i=1}^j |\psi_i\rangle \langle \psi_i| t} e^{-i\sum_{i=j+1}^N |\psi_i\rangle \langle \psi_i| t}||^2}$ . While in NDD region, each eigenstate therein is independent of arbitrary other one, producing the long range by system-size-independent correlations. The most significant feature of this region is the two parallel by separated boundaries in echo spectrum. This is a special region where the gap is not supported by coherences and will not prohibit the global thermalization (when there are system-size-dependent correlations).



## VI. CONCLUSION

The steady state of *mm*-case (consistent with the open boundary condition) is only due to the skin effect, where the many-body state (without exponential localization) holds global fluctuation due to the Hermiticity and the long-time behavior can be well predicted by diagonalization. This is in contrast to the localized state in *sq*-case (consistent with the periodic boundary condition) where the single-particle eigenstates exponentially decay with the localization length independent of system size[10, 56, 94, 124, 125, 130], and thus the long-time behavior is harder to predict by approximately diagonalization due to the non-Hermiticity. Zeno effect and confined light cone[96, 131] are unique to the *sq* case, while Hilbert space fragmentation[121, 154] and linearized bosonization are unique to the *mm* case, and the topological islands[125] is unique to the intermedia regime with finite strength of disorder but not yet reaches the ensemble-averaged result. A similar study with the correspondence to quantum systems is available by, e.g., transverse-field Ising model[162], XXX spin model, or BoseHubbard model[161], where the ergodicity (late stage) and scrambling (early stage) of *sq*-case are shared by the qubit ladder and nonintegrable transverse-field Ising model, while the nonergodicity of *mm*-case is shared by the qubit chain and integrable XXX spin model. Also, a protocol similar to the continuous measurement which give rise to the diffusion is the collective jumps[168] where the collectiveness can be diagnosed by the enhanced entanglement. Intermediate cases is achievable through complex disorder patterns by turning the transverse and longitudinal magnetic fields where the scrambling occurs with temporal fluctuations suppressed by the disorders (ensemble average) and initial state becomes mixed up in a large subspace[162]. While the absence of scrambling in *mm*-case is due to the conservation of initial states and each subspace (block-diagonal unitary operator) owns a unique exponentially decaying behavior, analogy to the internal dynamics of black hole and local integrals of motion of many-body localization which suppress the scrambling and rise the fluctuations. Note that the constriction on Hilbert space of the *mm*-case should be distinguished from the restriction of Hilbert space in *sq*-case where for the latter it is implemented by the construction of, e.g., Dicke basis (classical mixture cause thermalization as guaranteed by the permutational symmetry) and reducing from the  $O(2^N)$  Hilbert space dimension to  $O(N)$  subspaces.

**Data Availability Statement:** The data that support the findings of this study are available within the article.



## VII. APPENDIX: STOCHASTIC EVOLUTION WITH MARKOVIAN AND NON-MARKOVIAN DYNAMICS

The numerical operator  $\sum_i L_i^\dagger L_i$  is commutes with the nondissipative (Hermitian system) Hamiltonian. Intriguing phenomenas, like superradiant burst[29] during the photon emission, arise by choosing a Hermitian dissipation or decoherence matrix  $\gamma$  with nonzero off-diagonal component. Note that this dissipation strength is related to local imaginary potential[104, 108, 122] (inversely proportional to the pulsed measurement period), and is also referred to as measurement rate (or measurement strength), or the non-Markovian/Markovian noise amplitude, and proportional to the system-bath coupling strength[139].

The system of *sq*-case in Born-Markovian approximation weakly couple to the non-Markovian thermalizing environments where the non-Markovian noise therein cause the dephasing and broadened distribution with long-range hopping. Also, the memory effect of non-Markovian environments contributes to the large dissipation and the preserving of entangled states within the system as well as the long-time destination to larger steady-state entanglement (compares to the Markovian environments where the Markovian noise mainly cause the fast fluctuations)[116, 120].

For non-Markovian dynamics non-local in time, the dynamics can no longer be described by Lindblad master equation and the corresponding stochastic Schrodinger equations can describes only the no-jump process (controlled dissipation), instead of the jump (unconditioned dissipations) upon a measurement record[34, 167]. There is finite detector bandwidth and noise-noise correlation due to the information backflows from environment to system (in contrast to the Markovian system with nonunitary Lindblad dynamics[116]), despite the description by Markovian master equation still hold on average[34]. A vanishingly small dissipative incoherent case  $\gamma \rightarrow 0$  is applied to non-Markovian dynamics to guarantees the fast relaxation and dependence on noise correlation time, in the absence of quantum jump [80, 90, 96, 102]. Thus, despite the coupling to the non-Markovian environments, the continuous measurement by homodyne or heterodyne detection can be realized in *sq*-case in Markovian limit (i.e., infinite bandwidth, infinite count rate, and perfect detector), where the large dissipation rate guarantees the thermal state and the loss of initial information due to the environment. In *sq*-case, the volume-law (saturated) entanglement in short-time (long-time) scale is dominated by the Markovian (non-Markovian) dynamics.

Differently, in *mm*-case, evolution of the system strongly coupled to a thermal reservoirs (Markovian environment) is well described by the Markovian Lindblad master equation, and the non-Markovian memory effect induced complex coherence pattern (the infinite bound states due to the dissipationless non-Markovian dynamics), whose backaction effect induce the oscillation in entanglement, and the steady state is possible only in long-time limit. Note that despite the strong system-bath coupling, the Markovian thermal environment equilibrium at a certain temperature initially coherent with the system (without the quantum correlation/entanglement) in a product form  $\rho_S \otimes \rho_E$ [102, 103]. In this case, the strong noise in Markovian (noisy) environments results in a long timescale of slow relaxation, and the long non-Markovian noise-noise correlation time (weak non-Markovian) within bath in fact has a indistinguishable effect with the Markovian white noise, where both give rise to the classical diffusion in the system. In interacting case, the dissipative interaction is represented by a decoherence matrix which push the system toward thermalization, In noninteracting limit,  $\gamma_0 = \gamma \mathbf{I}$  while in the all-to-all interacting limit (Dicke limit in canonical setting[32, 33, 168]),  $\gamma_D = |\sqrt{\gamma}\rangle\langle\sqrt{\gamma}|$ , with  $|\sqrt{\gamma}\rangle$  the vector consist only the element  $\sqrt{\gamma}$ . The vectors made of eigenvalues arranged in descending order for  $\gamma_D$  supermajorize that of  $\gamma_0$ .

In Markov limit where the equation of motion depends only on the nearest past time, the bath energy density becomes static and depends only on the dissipation rate, while the general non-Markovian processes involve the average over the whole past (the noise). In strong non-Markovianity limit, the bandwidth of bath spectral density distribution is vanishing small and results in band-gap structure in bath, where the dissipation (as well as the system-bath coupling) favors the coherent dynamics[47, 73]. For systems of non-Hermitian dynamics, like the *mm*-case, the superpositional coherences coexist with the nonequilibrium dynamics induced by system-bath coupling, and the bound states preclude the exponential decay as in single particle picture. Such nonequilibrium dynamics in a open system the delocalization coexist with the coherence-induced many-body dynamical localization contribute to the large fidelity and the stored quantum information that is robust against disorder (thermal noise).

In the absent of quantum jump (by postselection), the dynamics can be described by the Linbladian equation  $\frac{d}{dt}\rho = -i[H, \rho] - \sum_i \frac{\gamma_i}{2} \{L_i^\dagger L_i, \rho\} = -i(H_{\text{eff}}\rho - \rho H_{\text{eff}}^\dagger)$  with  $H_{\text{eff}} = H - i \sum_i \frac{\gamma_i}{2} L_i^\dagger L_i$ , where the imaginary part of no-jump measurement operator  $L_0 = (\gamma_0 dt)^{-1/2}(1 - iH_{\text{eff}}dt)$  only given by the Hamiltonian  $H$  which governs evolution of  $\rho$ . The measurement-induced back action  $i \sum_i \frac{\gamma_i}{2} L_i^\dagger L_i$  is due to the memory effect non-Markovian environment[139, 151] which may contains some unobservable degrees of freedom coupled to the system and cause the thermalization[151]. The Lindblad master equation consistent with the continuous limit of quantum channel[60, 75], or the Markovian equation of motion of density matrix[123]. The individual trajectories  $|\psi(t)\rangle = \frac{e^{-iH_{\text{eff}}t}|\psi_0\rangle}{\|e^{-iH_{\text{eff}}t}|\psi_0\rangle\|}$  have

the stochastic time evolution[34, 91] (expanded up to first order in infinitesimal measurement time  $dt$  during the monitoring)  $d|\psi(t)\rangle = (-iH - \sum_i \frac{\gamma_i}{2} L_i^\dagger L_i + \langle\psi(t)| \sum_i \frac{\gamma_i}{2} L_i^\dagger L_i |\psi(t)\rangle) |\psi(t)\rangle dt$  in the absence of detection of (local Poisson) quantum jump (photo emission). The existence of time-dependent term  $\langle\psi(t)| \sum_i \frac{\gamma_i}{2} L_i^\dagger L_i |\psi(t)\rangle$  within above equation is due to the time-dependent norm  $\|e^{-iH_{\text{eff}}t} |\psi_0\rangle\|$  where  $L_i^\dagger L_i$  and  $H$  are Hermitian but  $H_{\text{eff}}$  is non-Hermitian. In this case the measurement on a individual trajectory returns no result and the pure state  $|\psi(t)\rangle$  changes infinitesimally under the non-unitary evolution. In above Lindblad equation, the commutator is the unitary part which is related to the coherence, while the summation over quantum channel index is the dissipative part. When the quantum channel index also refers to the local site index, the system-bath coupling on these local sites will causes the exponential decaying in Lieb-Robinson velocity of local observable[72], and leads to exact ground-state in infinite time limit[82]. Such slow down of quantum information propagation in the delocalization (chaotic) phase is consistent with the effect of disorder[52, 86] and the exponential localization is in agree with the thermalization in single particle picture where the system-bath coupling in moderate strength results in a unique steady state without the memory of initial state information. While for strong system-bath coupling (dephasing), the rised purely classical dynamics will suppress the thermalization by diminishing the mutual information (quantum correlations)[28, 72]. Both the quantum information which propagating in fixed velocity against the effect of disorder, and the coherence in open many-body system coupled to Markovian bath, exhibit nonlocal nature, which dominates in the non-Hermitian system with superpositional coherence pattern as a mixed state (as long as there are more than one trajectory) whose trajectory-averaged time evolution of the density matrix under Lindblad master equation is conditioned to a certain number of quantum jumps between trajectories (a special case with null jumps is the non-Hermitian case where there is a single trajectory)[39, 60, 75, 76]. The nonlocal measurement applied on such nonequilibrium many-body system reveals the incompatibility with the single-particle picture (i.e., the no-click limit with rigorous bulk-edge correspondence) or the mean-field non-Hermitian dynamics where dissipative and decoherence dominate. The probe record of such quantum jumps in unfixed number is not known. This is consistent with the  $mm$ -case, where there are infinite bound states corresponding to the mode propagating in growing speed and not be bounded by Lieb-Robinson velocity (the exponentially decaying). Such information propagating could be carried by supersonic mode[75], or the fluctuation-suppressed quasiparticle mode[10].

For discontinuous measurement protocol, distinct to the Homodyne or Heterodyne continuous measurement, there are discrete countable conserved quantities, like photon, and the corresponding unconditional dissipative dynamics is described by the Lindblad master equation  $\frac{d}{dt}\rho = -i(H_{\text{eff}}\rho - \rho H_{\text{eff}}^\dagger) + \sum_i \gamma_i L_i \rho L_i^\dagger$ . For this protocol, despite there are allowed transitions between nonunitary and unitary evolutions by the absence and presence of quantum jump which return null and unit detection results (Poisson random stochastic increments), respectively, during an infinitesimal time interval, the system only exhibit jump evolution and never enters the regime of diffusive evolution, as described by the point-process stochastic Schrodinger equation (nonlinear in  $|\psi(t)\rangle$ ),

$$\begin{aligned} d|\psi(t)\rangle &= |\psi(t+dt)\rangle - |\psi(t)\rangle \\ &= -i \left( H_{\text{eff}} + \frac{i}{2} \sum_i \gamma_i \langle\psi(t)| L_i^\dagger L_i |\psi(t)\rangle \right) |\psi(t)\rangle dt + \sum_i \left( \frac{L_i}{\sqrt{\langle\psi(t)| L_i^\dagger L_i |\psi(t)\rangle}} - 1 \right) |\psi(t)\rangle dN_i(t), \end{aligned} \quad (4)$$

where the expectation (or ensemble average) on the Poisson random stochastic increment  $dN_i(t)$  is the Born probability for unit detection result, and is unknown until the measurements are done, which reads  $\mathbb{E}[dN_i(t)] = \langle\psi(t)| L_i^\dagger L_i |\psi(t)\rangle \gamma_i dt = \|L_i |\psi(t)\rangle\|^2 \gamma_i dt$ ,  $dN_i(t) dN_j(t) = \delta_{ij} dN_i(t)$ . This makes it unable to eliminate or multiply the noise[45, 91], and meanwhile, retains the Poissonian randomness, in construct to the Wiener process with Ito stochasticity. Up to large number limit where the homodyne scheme and quantum state diffusion are achieved, the Poisson  $dN_i$  is replaced by the multiplicative Gaussian Ito noise. The local (short-range) correlations in single-particle picture (closed system) corresponds to the quantity linear on the stochastic quantum states like the expectation in basis of stochastic states, and the absence of long-range order is consistent with the result of cluster decomposition[79, 80].

While the nonlocal correlations corresponds to the nonlinear one, like the von Neumann entropy and von Neumann correlation. Only the latter is free from Lieb-Robinson bound and deeply affected by the local quantum channel, e.g., the ensemble average over a large number of quantum jumps such that the local quantum channel has a large enough width to take effect while a narrow quantum channel (mixed state) is in the sense that it can be purified to a symmetric local unitary operator[78], and local correlations are avoided by the statistical mixture which generally corresponds to weak symmetry[39, 77, 78]. Also, this is also in agree with the suppression on area-law entanglement by the quantum jumps which plays the role of perturbation. Further, in the case neither dominated by the classical

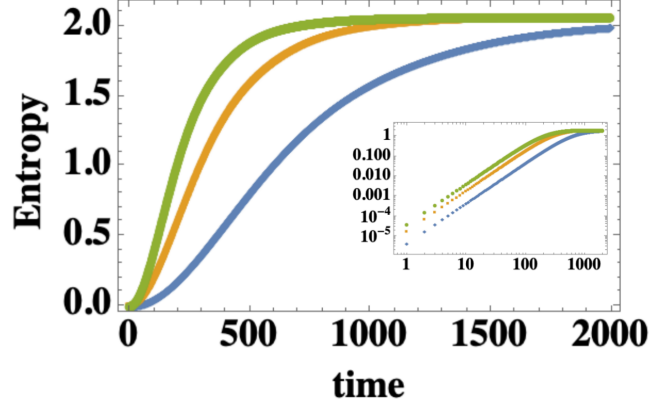


Figure 8. Von Neumann entropy  $S = -\ln \text{Tr}[(R_{sq}|\rho_0\rangle\langle\rho_0|)^2]$  for different system sizes.

dynamics or reaching the thermalization, the quantum information over large distance is allowed in inhomogeneous steady state with extensive long-range entanglement or the postquenched homogeneous integrable state[74].

### VIII. APPENDIX.B: EFFECT FROM LINDBLAD DYNAMICS TO $sq$ -CASE

For non-Hermitian and nonunitary observables  $O_{nH} = e^{-i\rho_{sq}t}$  ( $t \neq 0$ ),  $|\langle\rho_0|O_{nH}|\rho_0\rangle| = |\langle\rho'_0|R_{sq}|\rho_0\rangle| \approx |\langle\rho'_0|O_{nH}|\rho'_0\rangle|$ , and  $\langle\rho'_0|R_{sq}|\rho_0\rangle/\langle\rho'_0|\rho_0\rangle \neq 1$ , which means the effect of measurement apparatus keep finite but small during the evolution (also implies the perturbative treatment is invalid here). Then the effect of imaginary part related to the measurement-induced interaction can be estimated from the difference  $\langle\rho_0|O_{nH}|\rho_0\rangle - \langle\rho_0|UO_{nH}U^\dagger|\rho_0\rangle$  where  $U$  is nonunitary such that  $[O_{nH}, \ln U] \neq 0$  and  $\text{Tr}[UO_{nH}U^\dagger - O_{nH}] = 0$ .

We show the von Neumann entropy  $S = -\ln \text{Tr}[(R_{sq}|\rho_0\rangle\langle\rho_0|)^2]$  in Fig.8. Compares to the von Neumann entropy shown in Fig.1(a), we see that the peak at intermediate time vanishes and the entropy become monotonic and smooth over the whole evolution.

Next we consider the effect from weak interaction and the one body loss  $\gamma$ , which is also the decoherence function, the dynamics of time-dependent density  $R_{sq}$  can be described by the Lindblad function especially in long-time limit,

$$\frac{dR_{sq}}{dt} = -i(H_{int}R_{sq} - R_{sq}^\dagger H_{int}^\dagger) + \frac{\gamma}{2} \left( 2 \frac{\langle\rho_0|R_{sq}|\rho_0\rangle}{\langle\rho_0|\rho_0\rangle} \mathbf{I} - \{|\rho_0\rangle\langle\rho_0|, R_{sq}\} \right) + \frac{\gamma}{2} \left( 2 \frac{\langle\rho'_0|R_{sq}|\rho'_0\rangle}{\langle\rho'_0|\rho'_0\rangle} \mathbf{I} - \{|\rho'_0\rangle\langle\rho'_0|, R_{sq}\} \right), \quad (5)$$

where  $\mathbf{I}$  is the  $N \times N$  identity matrix, and the interacting Hamiltonian reads  $H_{int} = g|\rho_0\rangle\langle\rho'_0| + h.c..$  Then we numerically found that, the dynamics of expectation of  $\frac{\text{Tr}[|\rho_0\rangle\langle\rho_0|R_{sq}]}{\text{Tr}[|\rho_0\rangle\langle\rho_0|]} + (|\rho_0\rangle \leftrightarrow |\rho'_0\rangle)$  can be well described by

$$\begin{aligned} & \frac{\text{Tr}[|\rho_0\rangle\langle\rho_0|\dot{R}_{sq}]}{\text{Tr}[|\rho_0\rangle\langle\rho_0|]} + (|\rho_0\rangle \leftrightarrow |\rho'_0\rangle) \\ &= - \frac{ig\text{Tr}[|\rho_0\rangle\langle\rho_0|(|\rho_0\rangle\langle\rho'_0|R_{sq} - R_{sq}^\dagger|\rho'_0\rangle\langle\rho_0|)]}{\text{Tr}[|\rho_0\rangle\langle\rho_0|]} - \frac{ig\text{Tr}[|\rho'_0\rangle\langle\rho'_0|(|\rho_0\rangle\langle\rho'_0|R_{sq} - R_{sq}^\dagger|\rho'_0\rangle\langle\rho_0|)]}{\text{Tr}[|\rho'_0\rangle\langle\rho'_0|]} \\ & - \frac{ig\text{Tr}[|\rho_0\rangle\langle\rho_0|(|\rho'_0\rangle\langle\rho_0|R_{sq} - R_{sq}^\dagger|\rho_0\rangle\langle\rho'_0|)]}{\text{Tr}[|\rho_0\rangle\langle\rho_0|]} - \frac{ig\text{Tr}[|\rho'_0\rangle\langle\rho'_0|(|\rho'_0\rangle\langle\rho_0|R_{sq} - R_{sq}^\dagger|\rho_0\rangle\langle\rho'_0|)]}{\text{Tr}[|\rho'_0\rangle\langle\rho'_0|]} \\ & + \frac{\text{Tr}[|\rho_0\rangle\langle\rho_0|\frac{\gamma}{2} \left( 2 \frac{\langle\rho_0|R_{sq}|\rho_0\rangle}{\langle\rho_0|\rho_0\rangle} \mathbf{I} - \{|\rho_0\rangle\langle\rho_0|, R_{sq}\} \right)]}{\text{Tr}[|\rho_0\rangle\langle\rho_0|]} + \frac{\text{Tr}[|\rho'_0\rangle\langle\rho'_0|\frac{\gamma}{2} \left( 2 \frac{\langle\rho_0|R_{sq}|\rho_0\rangle}{\langle\rho_0|\rho_0\rangle} \mathbf{I} - \{|\rho_0\rangle\langle\rho_0|, R_{sq}\} \right)]}{\text{Tr}[|\rho'_0\rangle\langle\rho'_0|]} \\ & + \frac{\text{Tr}[|\rho'_0\rangle\langle\rho'_0|\frac{\gamma}{2} \left( 2 \frac{\langle\rho'_0|R_{sq}|\rho'_0\rangle}{\langle\rho'_0|\rho'_0\rangle} \mathbf{I} - \{|\rho'_0\rangle\langle\rho'_0|, R_{sq}\} \right)]}{\text{Tr}[|\rho'_0\rangle\langle\rho'_0|]} + \frac{\text{Tr}[|\rho_0\rangle\langle\rho_0|\frac{\gamma}{2} \left( 2 \frac{\langle\rho'_0|R_{sq}|\rho'_0\rangle}{\langle\rho'_0|\rho'_0\rangle} \mathbf{I} - \{|\rho'_0\rangle\langle\rho'_0|, R_{sq}\} \right)]}{\text{Tr}[|\rho_0\rangle\langle\rho_0|]}. \end{aligned} \quad (6)$$

We have the following relations at arbitrary  $t$ ,

$$\begin{aligned}
\frac{-i\text{Tr}[\rho_0 \langle \rho_0 | (|\rho_0 \rangle \langle \rho'_0| R_{sq} - R_{sq}^\dagger |\rho'_0 \rangle \langle \rho_0|)]}{\text{Tr}[\rho_0 \langle \rho_0|]} &= -i\text{Tr}[(|\rho_0 \rangle \langle \rho'_0| R_{sq} - R_{sq}^\dagger |\rho'_0 \rangle \langle \rho_0|)] = 2 \text{Im Tr}[\rho_0 \langle \rho'_0| R_{sq}], \\
\frac{-i\text{Tr}[\rho'_0 \langle \rho'_0 | (|\rho'_0 \rangle \langle \rho_0| R_{sq} - R_{sq}^\dagger |\rho_0 \rangle \langle \rho'_0|)]}{\text{Tr}[\rho'_0 \langle \rho'_0|]} &= -i\text{Tr}[(|\rho'_0 \rangle \langle \rho_0| R_{sq} - R_{sq}^\dagger |\rho_0 \rangle \langle \rho'_0|)] = 2 \text{Im Tr}[\rho'_0 \langle \rho_0| R_{sq}], \\
\frac{-i\text{Tr}[\rho_0 \langle \rho_0 | (|\rho'_0 \rangle \langle \rho_0| R_{sq} - R_{sq}^\dagger |\rho_0 \rangle \langle \rho'_0|)]}{\text{Tr}[\rho_0 \langle \rho_0|]} &= -i\text{Tr}[(|\rho_0 \rangle \langle \rho'_0| R_{sq} - R_{sq}^\dagger |\rho'_0 \rangle \langle \rho_0|)] = 2 \text{Im Tr}[\rho_0 \langle \rho'_0| R_{sq}], \\
\frac{-i\text{Tr}[\rho'_0 \langle \rho'_0 | (|\rho'_0 \rangle \langle \rho'_0| R_{sq} - R_{sq}^\dagger |\rho'_0 \rangle \langle \rho'_0|)]}{\text{Tr}[\rho'_0 \langle \rho'_0|]} &= -i\text{Tr}[(|\rho'_0 \rangle \langle \rho_0| R_{sq} - R_{sq}^\dagger |\rho_0 \rangle \langle \rho'_0|)] = 2 \text{Im Tr}[\rho'_0 \langle \rho_0| R_{sq}].
\end{aligned} \tag{7}$$

Note that  $\text{Im Tr}[\rho_0 \langle \rho'_0| R_{sq}] = -\text{Im Tr}[\rho'_0 \langle \rho_0| R_{sq}]$ .

At long-time where  $U_{sq}$  is trace preserving and  $1/\text{Tr}[\rho_0 \langle \rho_0|] = 1/\text{Tr}[\rho'_0 \langle \rho'_0|] = 1/N$ , there is symmetry for the exchange between states before and after measurement,

$$\begin{aligned}
\frac{\text{Tr}[\rho_0 \langle \rho_0| \frac{1}{2} \left( 2 \frac{\langle \rho_0 | R_{sq} | \rho_0 \rangle}{\langle \rho_0 | \rho_0 \rangle} \mathbf{I} - \{|\rho_0 \rangle \langle \rho_0|, R_{sq}\} \right)]}{\text{Tr}[\rho_0 \langle \rho_0|] (\text{Tr}[\rho_0 \langle \rho_0|] - 1)} &= \frac{\text{Tr}[\rho'_0 \langle \rho'_0| \frac{1}{2} \left( 2 \frac{\langle \rho'_0 | R_{sq} | \rho'_0 \rangle}{\langle \rho'_0 | \rho'_0 \rangle} \mathbf{I} - \{|\rho'_0 \rangle \langle \rho'_0|, R_{sq}\} \right)]}{\text{Tr}[\rho'_0 \langle \rho'_0|] (\text{Tr}[\rho'_0 \langle \rho'_0|] - 1)} = -\frac{\text{Tr}[\rho_0 \langle \rho_0| R_{sq}]}{\text{Tr}[\rho_0 \langle \rho_0|]} = -\frac{1}{N}, \\
\frac{\text{Tr}[\rho'_0 \langle \rho'_0| \frac{1}{2} \left( 2 \frac{\langle \rho_0 | R_{sq} | \rho_0 \rangle}{\langle \rho_0 | \rho_0 \rangle} \mathbf{I} - \{|\rho_0 \rangle \langle \rho_0|, R_{sq}\} \right)]}{\text{Tr}[\rho'_0 \langle \rho'_0|]} &= \frac{\text{Tr}[\rho_0 \langle \rho_0| \frac{1}{2} \left( 2 \frac{\langle \rho'_0 | R_{sq} | \rho'_0 \rangle}{\langle \rho'_0 | \rho'_0 \rangle} \mathbf{I} - \{|\rho'_0 \rangle \langle \rho'_0|, R_{sq}\} \right)]}{\text{Tr}[\rho_0 \langle \rho_0|]} = \frac{\text{Tr}[\rho_0 \langle \rho_0| R_{sq}]}{2\text{Tr}[\rho_0 \langle \rho_0|]} = \frac{1}{2N},
\end{aligned} \tag{8}$$

Note the following relations,

$$\begin{aligned}
\frac{\text{Tr}[R_{sq}]}{N} &= \frac{\text{Tr}[\rho_0 \langle \rho_0| R_{sq}]}{\text{Tr}[\rho_0 \langle \rho_0|]} = \frac{\text{Tr}[\rho'_0 \langle \rho'_0| R_{sq}]}{\text{Tr}[\rho'_0 \langle \rho'_0|]} = \frac{\text{Tr}[\rho_0 \langle \rho'_0| \rho'_0 \langle \rho_0| R_{sq}]}{N^2} \\
&= -\frac{\text{Tr}[\rho_0 \langle \rho_0| \frac{1}{2} \left( 2 \frac{\langle \rho_0 | R_{sq} | \rho_0 \rangle}{\langle \rho_0 | \rho_0 \rangle} \mathbf{I} - \{|\rho_0 \rangle \langle \rho_0|, R_{sq}\} \right)]}{\text{Tr}[\rho_0 \langle \rho_0|] (\text{Tr}[\rho_0 \langle \rho_0|] - 1)} = -\frac{\text{Tr}[\rho'_0 \langle \rho'_0| \frac{1}{2} \left( 2 \frac{\langle \rho'_0 | R_{sq} | \rho'_0 \rangle}{\langle \rho'_0 | \rho'_0 \rangle} \mathbf{I} - \{|\rho'_0 \rangle \langle \rho'_0|, R_{sq}\} \right)]}{\text{Tr}[\rho'_0 \langle \rho'_0|] (\text{Tr}[\rho'_0 \langle \rho'_0|] - 1)} \sim e^{-t}, \tag{9} \\
\| |\rho_0 \rangle \langle \rho_0| \|_2 &= \| |\rho'_0 \rangle \langle \rho'_0| \|_2 = \| |\rho_0 \rangle \langle \rho'_0| \|_2 = \| |\rho'_0 \rangle \langle \rho_0| \|_2 = \frac{1}{N} \| |\rho_0 \rangle \langle \rho'_0| \rho'_0 \langle \rho_0| \|_2 \\
&= \text{Tr}[\rho_0 \langle \rho_0|] = \text{Tr}[\rho'_0 \langle \rho'_0|] = N \ (\forall t),
\end{aligned}$$

as shown in Fig.9(a) where  $\langle R_{sq} \rangle_1$ ,  $\langle R_{sq} \rangle_2$ ,  $\langle \mathcal{D} \rangle_1$  represent the second, third, and fourth term of the first expression of Eq.9. While  $\langle R_{sq} \rangle_3 := \frac{1}{N} \text{Tr}[\rho_0 \langle \rho'_0| R_{sq}]$  and  $\langle R_{sq} \rangle_4 := \frac{\text{Tr}[\rho_0 \langle \rho'_0| R_{sq}]}{\text{Tr}[\rho_0 \langle \rho'_0|]}$  are shown in Fig.9(a)-(b). At long-time where  $U_{sq}$  still be trace preserving,

$$\frac{\text{Tr}[\rho_0 \langle \rho_0| R_{sq}]}{\text{Tr}[\rho_0 \langle \rho_0|]} = \frac{\text{Tr}[\rho'_0 \langle \rho'_0| R_{sq}]}{\text{Tr}[\rho'_0 \langle \rho'_0|]} = \frac{\text{Tr}[\rho'_0 \langle \rho_0| R_{sq}]}{\| |\rho'_0 \rangle \langle \rho_0| \|_2} = \frac{\text{Tr}[\rho_0 \langle \rho'_0| R_{sq}]}{\| |\rho_0 \rangle \langle \rho'_0| \|_2} = \frac{1}{N}, \tag{10}$$

where the 2-norm and trace norm satisfy  $\| |\rho_0 \rangle \langle \rho'_0| \|_2 = 2 \| |\rho_0 \rangle \langle \rho'_0| \|_{tr} = N$ .

While at long-time limit  $t \rightarrow \infty$  where  $U_{sq}$  is nomore trace preserving and  $1/\text{Tr}[\rho_0 \langle \rho_0|] = 1/N$ ,  $1/\text{Tr}[\rho'_0 \langle \rho'_0|] = 0$ ,

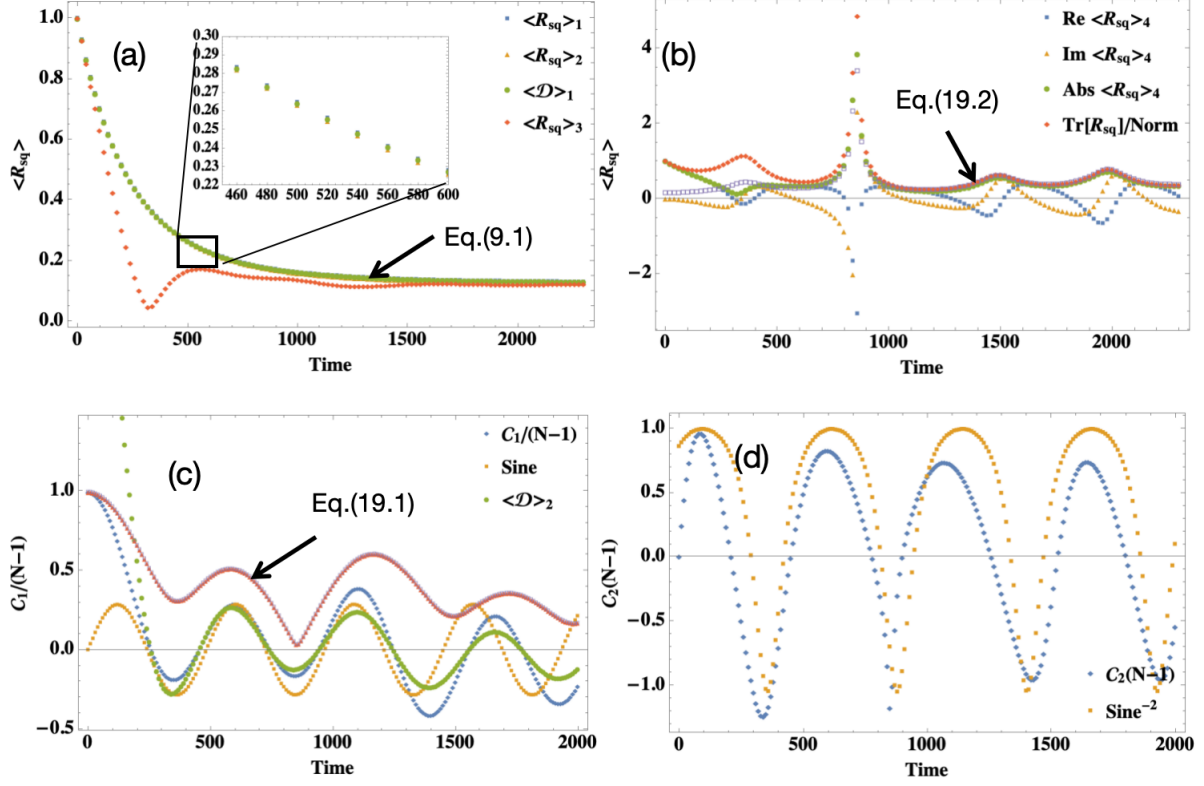


Figure 9. (a) Blue, orange and green dots represent the expectations  $\frac{\text{Tr}[\rho_0 \langle \rho_0 | R_{sq} \rangle]}{\text{Tr}[\rho_0 \langle \rho_0 |]}$ ,  $\frac{\text{Tr}[\rho'_0 \langle \rho'_0 | R_{sq} \rangle]}{\text{Tr}[\rho'_0 \langle \rho'_0 |]}$  and  $\left| \frac{\text{Tr}[\rho'_0 \langle \rho_0 | R_{sq} \rangle]}{\|[\rho'_0 \langle \rho_0 |]\|_2} \right|$ , respectively. (b) Blue, orange and green dots represent the real part, imaginary part, and absolute value of  $\frac{\text{Tr}[\rho'_0 \langle \rho_0 | R_{sq} \rangle]}{\text{Tr}[\rho'_0 \langle \rho_0 |]}$ .

we have

$$\begin{aligned}
 \frac{\text{Tr}[\rho_0 \langle \rho_0 | \frac{1}{2} \left( 2 \frac{\langle \rho_0 | R_{sq} | \rho_0 \rangle}{\langle \rho_0 | \rho_0 \rangle} \mathbf{I} - \{ |\rho_0 \rangle \langle \rho_0 |, R_{sq} \} \right)]}{\text{Tr}[\rho_0 \langle \rho_0 |] (\text{Tr}[\rho_0 \langle \rho_0 |] - 1)} &= -\frac{1}{N}, \\
 \frac{\text{Tr}[\rho'_0 \langle \rho'_0 | \frac{1}{2} \left( 2 \frac{\langle \rho_0 | R_{sq} | \rho_0 \rangle}{\langle \rho_0 | \rho_0 \rangle} \mathbf{I} - \{ |\rho_0 \rangle \langle \rho_0 |, R_{sq} \} \right)]}{\text{Tr}[\rho'_0 \langle \rho'_0 |]} &= \frac{\text{Tr}[\rho_0 \langle \rho_0 | R_{sq} \rangle]}{\text{Tr}[\rho_0 \langle \rho_0 |]} = \frac{1}{N}, \\
 \frac{\text{Tr}[\rho'_0 \langle \rho'_0 | \frac{1}{2} \left( 2 \frac{\langle \rho'_0 | R_{sq} | \rho'_0 \rangle}{\langle \rho'_0 | \rho'_0 \rangle} \mathbf{I} - \{ |\rho'_0 \rangle \langle \rho'_0 |, R_{sq} \} \right)]}{\text{Tr}[\rho'_0 \langle \rho'_0 |] (\text{Tr}[\rho'_0 \langle \rho'_0 |] - 1)} &= 0, \\
 \frac{\text{Tr}[\rho_0 \langle \rho_0 | \frac{1}{2} \left( 2 \frac{\langle \rho'_0 | R_{sq} | \rho'_0 \rangle}{\langle \rho'_0 | \rho'_0 \rangle} \mathbf{I} - \{ |\rho'_0 \rangle \langle \rho'_0 |, R_{sq} \} \right)]}{\text{Tr}[\rho_0 \langle \rho_0 |]} &= \infty,
 \end{aligned} \tag{11}$$

To obtain a long-time-stable result, we restrict the dissipative part of the dynamics of  $R_{sq}$  (Eq.(5)) to only containing the state before nonunitary evolution (measurement), i.e.,  $|\rho_0\rangle$ . then we have

$$\lim_{t \rightarrow \infty} \left[ \frac{\text{Tr}[\rho_0 \langle \rho_0 | \dot{R}_{sq}]}{\text{Tr}[\rho_0 \langle \rho_0 |]} + (|\rho_0\rangle \leftrightarrow |\rho'_0\rangle) \right] = \gamma \frac{2-N}{N}, \tag{12}$$

which is nearly  $-\gamma$  in the large- $N$  limit. The long-time limit of  $\frac{\text{Tr}[\rho_0 \langle \rho_0 | \dot{R}_{sq}]}{\text{Tr}[\rho_0 \langle \rho_0 |]}$  turns to be the same result. This result is consistent with Refs.[], such that the dissipative part of the dynamics will not generates time-dependence to the postselection probability at long-time limit, as long as the decoherence function is time-independent.



Next we consider the effect from Lindblad dynamics to the time evolution of von Neumann entropy  $S = -\ln \text{Tr}[(R_{sq}|\rho_0\rangle\langle\rho_0|)^2]$ ,

$$\begin{aligned}\dot{S} &= \frac{-1}{\text{Tr}[(R_{sq}|\rho_0\rangle\langle\rho_0|)^2]} \text{Tr}\left[\frac{dR_{sq}}{dt}|\rho_0\rangle\langle\rho_0|R_{sq}|\rho_0\rangle\langle\rho_0| + R_{sq}|\rho_0\rangle\langle\rho_0|\frac{dR_{sq}}{dt}|\rho_0\rangle\langle\rho_0|\right] \\ &= \frac{-2}{\text{Tr}[(R_{sq}|\rho_0\rangle\langle\rho_0|)^2]} \text{Tr}\left[\frac{dR_{sq}}{dt}|\rho_0\rangle\langle\rho_0|R_{sq}|\rho_0\rangle\langle\rho_0|\right].\end{aligned}\quad (13)$$

We found that the unitary part in the Lindblad function shows to be irrelevant to introduce large randomness determined by the interaction strength  $g$ , thus here we consider only the role of dissipative part, i.e.,  $g \ll \gamma$ . Then we define

$$\begin{aligned}f_1 &:= \text{Tr}\left[\frac{1}{2}\left(2\frac{\langle\rho_0|R_{sq}|\rho_0\rangle}{\langle\rho_0|\rho_0\rangle}\mathbf{I} - \{|\rho_0\rangle\langle\rho_0|, R_{sq}\}\right)|\rho_0\rangle\langle\rho_0|R_{sq}|\rho_0\rangle\langle\rho_0|\right], \\ f_2 &:= \text{Tr}\left[\frac{1}{2}\left(2\frac{\langle\rho'_0|R_{sq}|\rho'_0\rangle}{\langle\rho'_0|\rho'_0\rangle}\mathbf{I} - \{|\rho'_0\rangle\langle\rho'_0|, R_{sq}\}\right)|\rho_0\rangle\langle\rho_0|R_{sq}|\rho_0\rangle\langle\rho_0|\right], \\ f_3 &:= \text{Tr}[(R_{sq}|\rho_0\rangle\langle\rho_0|)^2].\end{aligned}\quad (14)$$

As shown in Fig.10,  $f_1$  exhibits the same exponential decay with  $f_3$ , while  $f_2$  decay with fluctuations, and  $f_2$  is bound by  $f_1$  from below. Further, we found that, by renormalizing the functions such that their initial value equals 1, we have  $\tilde{f}_1 = \tilde{f}_3$ . Thus the  $f_1$  does not contributions to the time-dependence of the entropy, while  $f_2$  solely leads to fluctuations with decaying amplitude. Roughly speaking,  $\langle\rho'_0|\rho_0\rangle$  contributes to the fluctuation last for a long time (as long as  $U_{sq}$  be trace preserving), while  $\langle\rho'_0|\rho'_0\rangle$  and  $\langle\rho_0|\rho_0\rangle$  contribute to the exponential decay with time. To understand this, we consider the correlation function between the two states (before and after measurement)

$$\mathcal{C}_1(t) := \text{Re}\left(\frac{\text{Tr}[|\rho_0\rangle\langle\rho_0|\rho'_0\rangle\langle\rho'_0|R_{sq}]}{\text{Tr}[R_{sq}]} - \frac{\text{Tr}[|\rho_0\rangle\langle\rho_0|R_{sq}]}{\text{Tr}[R_{sq}]} \frac{\text{Tr}[|\rho'_0\rangle\langle\rho'_0|R_{sq}]}{\text{Tr}[R_{sq}]}\right) = \text{Re}\frac{\text{Tr}[|\rho_0\rangle\langle\rho_0|\rho'_0\rangle\langle\rho'_0|R_{sq}]}{\text{Tr}[R_{sq}]} - 1, \quad (15)$$

where  $\frac{\text{Tr}[|\rho_0\rangle\langle\rho_0|R_{sq}]}{\text{Tr}[R_{sq}]} = \frac{\text{Tr}[|\rho'_0\rangle\langle\rho'_0|R_{sq}]}{\text{Tr}[R_{sq}]} = 1$  and thus  $\mathcal{C}_1(0) = N - 1$ . We found that, in the late-time stage,

$$\mathcal{C}_1(t) \approx -2 \frac{\text{Tr}[|\rho'_0\rangle\langle\rho'_0|\left(2\frac{\langle\rho_0|R_{sq}|\rho_0\rangle}{\langle\rho_0|\rho_0\rangle}\mathbf{I} - \{|\rho_0\rangle\langle\rho_0|, R_{sq}\}\right)]}{\text{Tr}[|\rho'_0\rangle\langle\rho'_0|]} = -2 \frac{\text{Tr}[|\rho_0\rangle\langle\rho_0|\left(2\frac{\langle\rho'_0|R_{sq}|\rho'_0\rangle}{\langle\rho'_0|\rho'_0\rangle}\mathbf{I} - \{|\rho'_0\rangle\langle\rho'_0|, R_{sq}\}\right)]}{\text{Tr}[|\rho_0\rangle\langle\rho_0|]} \sim \alpha \sin(\beta t), \quad (16)$$

which can be fitted by a sine function as shown in Fig.9(c). Here  $\alpha$  and  $\beta$  are the fitting parameters. We also consider the following correlation functions in variant form

$$\begin{aligned}\mathcal{C}_2(t) &:= \text{Re}\left(\frac{\text{Tr}[|\rho_0\rangle\langle\rho_0|\rho'_0\rangle\langle\rho'_0|R_{sq}]}{\| |\rho_0\rangle\langle\rho_0|\rho'_0\rangle\langle\rho'_0| \|_2} - \frac{\text{Tr}[|\rho_0\rangle\langle\rho_0|R_{sq}]}{\| |\rho_0\rangle\langle\rho_0| \|_2} \frac{\text{Tr}[|\rho'_0\rangle\langle\rho'_0|R_{sq}]}{\| |\rho'_0\rangle\langle\rho'_0| \|_2}\right) \sim \frac{-1}{\sin(\alpha t + \beta)^2}, \\ \mathcal{C}_3(t) &:= \text{Re}\left(\frac{\text{Tr}[|\rho_0\rangle\langle\rho_0|\rho'_0\rangle\langle\rho'_0|R_{sq}]}{\text{Tr}[|\rho_0\rangle\langle\rho_0|\rho'_0\rangle\langle\rho'_0|]} - \frac{\text{Tr}[|\rho_0\rangle\langle\rho_0|R_{sq}]}{\| |\rho_0\rangle\langle\rho_0| \|_2} \frac{\text{Tr}[|\rho'_0\rangle\langle\rho'_0|R_{sq}]}{\| |\rho'_0\rangle\langle\rho'_0| \|_2}\right) \sim \frac{-t}{\sin(\alpha t + \beta)^2},\end{aligned}\quad (17)$$

which can be fitted by the inverse squared sine function as shown in Fig.9(d). Using the identity

$$|\text{Tr}[\cdot]| = \frac{\|(\cdot)^2\|_2}{\|\cdot\|_2}, \quad (18)$$

we can obtain following relations,

$$\begin{aligned}\| |\rho_0\rangle\langle\rho_0|\rho'_0\rangle\langle\rho'_0| \|_2 &= \| |\rho_0\rangle\langle\rho'_0| \|_2 \|\text{Tr}[|\rho_0\rangle\langle\rho'_0|]\| = N \|\text{Tr}[|\rho_0\rangle\langle\rho'_0|]\| = N \|\text{Tr}[|\rho'_0\rangle\langle\rho_0|]\|, \\ \frac{\text{Tr}[R_{sq}]}{\| |\rho_0\rangle\langle\rho_0|\rho'_0\rangle\langle\rho'_0| \|_2} &\approx \frac{1}{N} \left| \frac{\text{Tr}[|\rho_0\rangle\langle\rho'_0|R_{sq}]}{\text{Tr}[|\rho_0\rangle\langle\rho'_0|]} \right| = \frac{1}{N} \left| \left( \frac{\text{Tr}[|\rho'_0\rangle\langle\rho_0|R_{sq}]}{\text{Tr}[|\rho'_0\rangle\langle\rho_0|]} \right)^* \right| \approx \frac{1}{N^2} \frac{(\| |\rho_0\rangle\langle\rho_0|\rho'_0\rangle\langle\rho'_0| \|_2)^2}{(\| |\rho_0\rangle\langle\rho_0|\rho'_0\rangle\langle\rho'_0| \|_2)^2}\end{aligned}\quad (19)$$

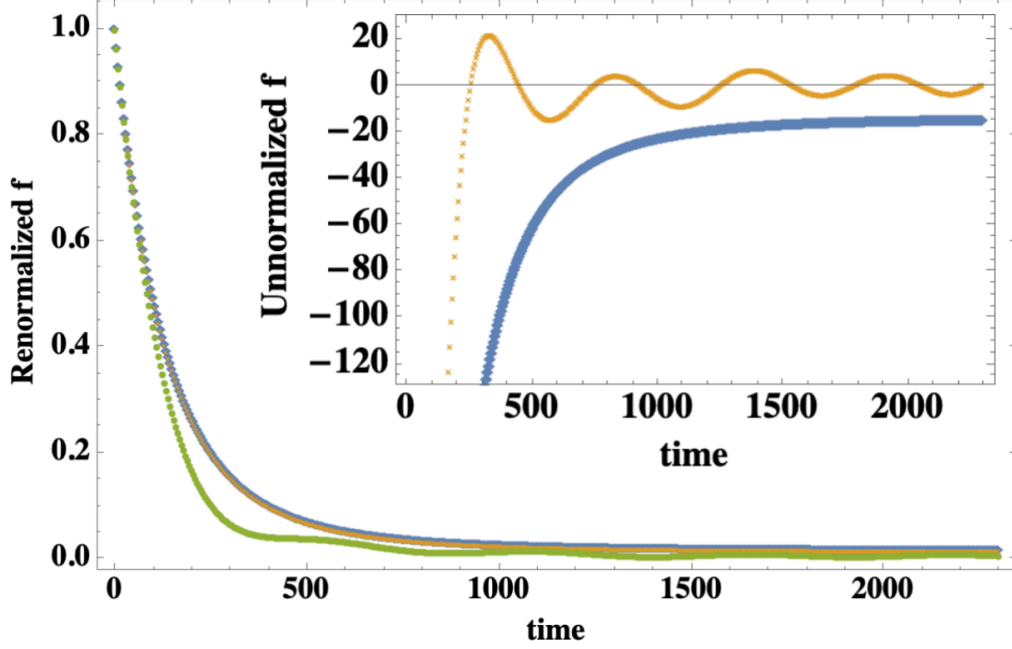


Figure 10. The blue, orange and green dots represent the renormalized functions  $\tilde{f}_1$ ,  $\tilde{f}_3$ , and  $\widetilde{f_1 + f_2}$ , respectively. The inset show the unnormalized functions  $f_1$  (blue) and  $f_2$  (orange).

we have

$$\begin{aligned}
 \mathcal{C}_2(t) &= (\mathcal{C}_1(t) + 1) \frac{\text{Tr}[R_{sq}]}{\| |\rho_0\rangle\langle\rho_0|\rho'_0\rangle\langle\rho'_0| \|_2} - \frac{\text{Tr}[|\rho_0\rangle\langle\rho_0|R_{sq}]}{\text{Tr}[|\rho_0\rangle\langle\rho_0|]} \frac{\text{Tr}[|\rho'_0\rangle\langle\rho'_0|R_{sq}]}{\text{Tr}[|\rho'_0\rangle\langle\rho'_0|]} \\
 &\approx \frac{1}{N} (\mathcal{C}_1(t) + 1) \left| \frac{\text{Tr}[|\rho_0\rangle\langle\rho'_0|R_{sq}]}{\text{Tr}[|\rho_0\rangle\langle\rho'_0|]} \right| - \left( \frac{\text{Tr}[|\rho_0\rangle\langle\rho_0|R_{sq}]}{\text{Tr}[|\rho_0\rangle\langle\rho_0|]} \right)^2 \sim \frac{\partial^2 \ln \mathcal{C}_1(t)}{\partial \mathcal{C}_1(t)^2}, \\
 \mathcal{C}_3(t) &\approx (\mathcal{C}_2(t) + \left( \frac{\text{Tr}[|\rho_0\rangle\langle\rho_0|R_{sq}]}{\text{Tr}[|\rho_0\rangle\langle\rho_0|]} \right)^2) \frac{(\| |\rho_0\rangle\langle\rho_0|\rho'_0\rangle\langle\rho'_0| \|_2)^2}{(\| |\rho_0\rangle\langle\rho_0|\rho'_0\rangle\langle\rho'_0| \|_2)^2} \sim \mathcal{C}_2(t)t.
 \end{aligned} \tag{20}$$

Next we consider the off-diagonal term of the population, in which case the dissipative part reads

$$\frac{\gamma}{2} \left( 2 \frac{\langle\rho'_0|R_{sq}|\rho_0\rangle}{\langle\rho'_0|\rho_0\rangle} \mathbf{I} - \frac{\{|\rho'_0\rangle\langle\rho_0|, R_{sq}\}}{\langle\rho_0|\rho'_0\rangle} \right) + (|\rho_0\rangle \leftrightarrow |\rho'_0\rangle). \tag{21}$$

Then by estimating its expectation on the states before and after the measurement, we obtain

$$\begin{aligned}
 \frac{\text{Tr}[\frac{1}{2} (2 \frac{\langle\rho'_0|R_{sq}|\rho_0\rangle}{\langle\rho'_0|\rho_0\rangle} \mathbf{I} - \frac{\{|\rho_0\rangle\langle\rho'_0|, R_{sq}\}}{\langle\rho'_0|\rho_0\rangle}) |\rho_0\rangle\langle\rho_0|]}{\text{Tr}[|\rho_0\rangle\langle\rho_0|]} &= \frac{\text{Tr}[\frac{1}{2} (2 \frac{\langle\rho_0|R_{sq}|\rho'_0\rangle}{\langle\rho_0|\rho'_0\rangle} \mathbf{I} - \frac{\{|\rho'_0\rangle\langle\rho_0|, R_{sq}\}}{\langle\rho_0|\rho'_0\rangle}) |\rho_0\rangle\langle\rho_0|]}{\text{Tr}[|\rho_0\rangle\langle\rho_0|]}, \\
 \frac{\text{Tr}[\frac{1}{2} (2 \frac{\langle\rho'_0|R_{sq}|\rho_0\rangle}{\langle\rho'_0|\rho_0\rangle} \mathbf{I} - \frac{\{|\rho_0\rangle\langle\rho'_0|, R_{sq}\}}{\langle\rho'_0|\rho_0\rangle}) |\rho'_0\rangle\langle\rho'_0|]}{\text{Tr}[|\rho'_0\rangle\langle\rho'_0|]} &= \frac{\text{Tr}[\frac{1}{2} (2 \frac{\langle\rho_0|R_{sq}|\rho'_0\rangle}{\langle\rho_0|\rho'_0\rangle} \mathbf{I} - \frac{\{|\rho'_0\rangle\langle\rho_0|, R_{sq}\}}{\langle\rho_0|\rho'_0\rangle}) |\rho'_0\rangle\langle\rho'_0|]}{\text{Tr}[|\rho'_0\rangle\langle\rho'_0|]}.
 \end{aligned} \tag{22}$$

Further, the expectations on the states before and after the measurement converge to a stable difference as long as  $U_{sq}$  is trace preserving,

$$f_4 := \frac{\text{Tr}[(2 \frac{\langle\rho'_0|R_{sq}|\rho_0\rangle}{\langle\rho'_0|\rho_0\rangle} \mathbf{I} - \frac{\{|\rho_0\rangle\langle\rho'_0|, R_{sq}\}}{\langle\rho'_0|\rho_0\rangle}) |\rho'_0\rangle\langle\rho'_0|]}{\text{Tr}[|\rho'_0\rangle\langle\rho'_0|]} - \frac{\text{Tr}[(2 \frac{\langle\rho_0|R_{sq}|\rho'_0\rangle}{\langle\rho_0|\rho'_0\rangle} \mathbf{I} - \frac{\{|\rho'_0\rangle\langle\rho_0|, R_{sq}\}}{\langle\rho_0|\rho'_0\rangle}) |\rho_0\rangle\langle\rho_0|]}{\text{Tr}[|\rho_0\rangle\langle\rho_0|]} \rightarrow \frac{1}{2^N}, \tag{23}$$

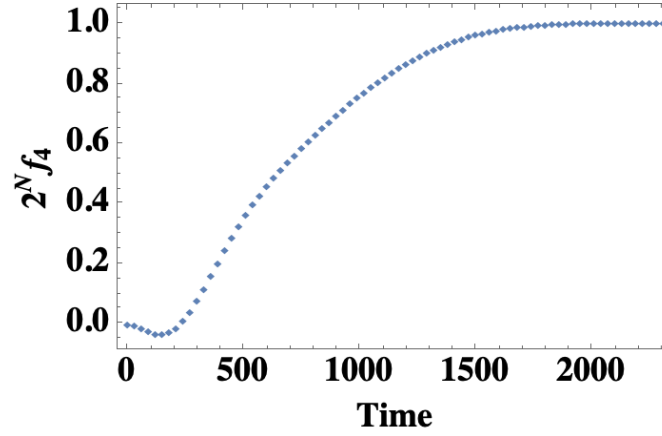


Figure 11. Eq.(23).

which vanish in the large- $N$  limit.

- 
- [1] Sahoo, Sharmistha, et al. "Traversable wormhole and Hawking-Page transition in coupled complex SYK models." *Physical Review Research* 2.4 (2020): 043049.
  - [2] Cao, Zan, Zhenyu Xu, and Adolfo del Campo. "Probing quantum chaos in multipartite systems." *Physical Review Research* 4.3 (2022): 033093.
  - [3] Choi, Soonwon, et al. "Emergent SU (2) dynamics and perfect quantum many-body scars." *Physical review letters* 122.22 (2019): 220603.
  - [4] Turner, C.J., Michailidis, A.A., Abanin, D.A. et al. Weak ergodicity breaking from quantum many-body scars. *Nature Phys* 14, 745–749 (2018). <https://doi.org/10.1038/s41567-018-0137-5>
  - [5] Anza, Fabio, Christian Gogolin, and Marcus Huber. "Eigenstate thermalization for degenerate observables." *Physical Review Letters* 120.15 (2018): 150603.
  - [6] Tian, Peng, Roman Riser, and Eugene Kanzieper. "Statistics of local level spacings in single-and many-body quantum chaos." *Physical Review Letters* 132.22 (2024): 220401.
  - [7] Mondaini, Rubem, and Marcos Rigol. "Eigenstate thermalization in the two-dimensional transverse field Ising model. II. Off-diagonal matrix elements of observables." *Physical Review E* 96.1 (2017): 012157.
  - [8] D'Alessio, Luca, et al. "From quantum chaos and eigenstate thermalization to statistical mechanics and thermodynamics." *Advances in Physics* 65.3 (2016): 239-362.
  - [9] Rigol, Marcos, Vanja Dunjko, and Maxim Olshanii. "Thermalization and its mechanism for generic isolated quantum systems." *Nature* 452.7189 (2008): 854-858.
  - [10] Cecile, Guillaume, Jacopo De Nardis, and Enej Ilievski. "Squeezed ensembles and anomalous dynamic roughening in interacting integrable chains." *Physical Review Letters* 132.13 (2024): 130401.
  - [11] Linden, Noah, et al. "Quantum mechanical evolution towards thermal equilibrium." *Physical Review E—Statistical, Nonlinear, and Soft Matter Physics* 79.6 (2009): 061103.
  - [12] Matsoukas-Roubeas, Apollonas S., et al. "Non-Hermitian Hamiltonian deformations in quantum mechanics." *Journal of High Energy Physics* 2023.1 (2023): 1-31.
  - [13] Hamazaki, Ryusuke, Kohei Kawabata, and Masahito Ueda. "Non-Hermitian many-body localization." *Physical review letters* 123.9 (2019): 090603.
  - [14] Midya, Bikashkali. "Topological phase transition in fluctuating imaginary gauge fields." *Physical Review A* 109.6 (2024): L061502.
  - [15] Cheng, Jun-Qing, Shuai Yin, and Dao-Xin Yao. "Dynamical localization transition in the non-Hermitian lattice gauge theory." *Communications Physics* 7.1 (2024): 58.
  - [16] Onizhuk, Mykyta, et al. "Understanding central spin decoherence due to interacting dissipative spin baths." *Physical Review Letters* 132.25 (2024): 250401.
  - [17] Zhang, Yuxuan, Juan Carrasquilla, and Yong Baek Kim. "Observation of a non-Hermitian supersonic mode." *arXiv preprint arXiv:2406.15557* (2024).
  - [18] Shen, Huitao, Bo Zhen, and Liang Fu. "Topological band theory for non-Hermitian Hamiltonians." *Physical review letters* 120.14 (2018): 146402.
  - [19] Linden, Noah, et al. "Quantum mechanical evolution towards thermal equilibrium." *Physical Review E—Statistical,*

- Nonlinear, and Soft Matter Physics 79.6 (2009): 061103.
- [20] Moharramipour, Amin, et al. "Symmetry enforced entanglement in maximally mixed states." arXiv preprint arXiv:2406.08542 (2024).
  - [21] Popescu, Sandu, Anthony J. Short, and Andreas Winter. "Entanglement and the foundations of statistical mechanics." *Nature Physics* 2.11 (2006): 754-758.
  - [22] Anza, Fabio, Christian Gogolin, and Marcus Huber. "Eigenstate thermalization for degenerate observables." *Physical Review Letters* 120.15 (2018): 150603.
  - [23] Pulikkottil, Jethin J., et al. "Entanglement production by interaction quenches of quantum chaotic subsystems." *Physical Review E* 101.3 (2020): 032212.
  - [24] Nielsen, Michael A., and Guifr  Vidal. "Majorization and the interconversion of bipartite states." *Quantum Inf. Comput.* 1.1 (2001): 76-93.
  - [25] Allahverdyan, Armen E., Roger Balian, and Th M. Nieuwenhuizen. "Maximal work extraction from finite quantum systems." *Europhysics Letters* 67.4 (2004): 565.
  - [26] F. Verstraete, M. M. Wolf, and J. Ignacio Cirac, Quantum computation and quantum-state engineering driven by dissipation, *Nature Physics* 5, 633 (2009).
  - [27] de Vicente, Julio I., Cornelia Spee, and Barbara Kraus. "Maximally entangled set of multipartite quantum states." *Physical review letters* 111.11 (2013): 110502.
  - [28] Wang, Yu-Peng, Chen Fang, and Jie Ren. "Absence of measurement-induced entanglement transition due to feedback-induced skin effect." *Physical Review B* 110.3 (2024): 035113.
  - [29] Mok, Wai-Keong, et al. "Dicke superradiance requires interactions beyond nearest neighbors." *Physical Review Letters* 130.21 (2023): 213605.
  - [30] Moharramipour, Amin, et al. "Symmetry enforced entanglement in maximally mixed states." arXiv preprint arXiv:2406.08542 (2024).
  - [31] Diosi, Lajos, Nicolas Gisin, and Walter T. Strunz. "Non-Markovian quantum state diffusion." *Physical Review A* 58.3 (1998): 1699.
  - [32] R. H. Dicke, Coherence in spontaneous radiation processes, *Phys. Rev.* 93, 99 (1954).
  - [33] Defenu, Nicol , David Mukamel, and Stefano Ruffo. "Ensemble inequivalence in long-range quantum systems." *Physical Review Letters* 133.5 (2024): 050403.
  - [34] Barchielli, Alberto, and Matteo Gregoratti. *Quantum trajectories and measurements in continuous time: the diffusive case*. Vol. 782. Springer Science & Business Media, 2009.
  - [35] Bulgac, Aurel, Matthew Kafker, and Ibrahim Abdurrahman. "Measures of complexity and entanglement in many-fermion systems." *Physical Review C* 107.4 (2023): 044318.
  - [36] Seif, Alireza, et al. "Measurement and Feed Forward Induced Entanglement Negativity Transition." *Physical Review Letters* 133.5 (2024): 050402.
  - [37] Minganti, Fabrizio, et al. "Spectral theory of Liouvillians for dissipative phase transitions." *Physical Review A* 98.4 (2018): 042118.
  - [38] Agarwal, Lakshya, Subhayan Sahu, and Shenglong Xu. "Charge transport, information scrambling and quantum operator-coherence in a many-body system with U (1) symmetry." *Journal of High Energy Physics* 2023.5 (2023): 1-33.
  - [39] Van Regemortel, Mathias, et al. "Entanglement entropy scaling transition under competing monitoring protocols." *Physical Review Letters* 126.12 (2021): 123604.
  - [40] Wang, Zuo, Li-Jun Lang, and Liang He. "Emergent Mott insulators and non-Hermitian conservation laws in an interacting bosonic chain with noninteger filling and nonreciprocal hopping." *Physical Review B* 105.5 (2022): 054315.
  - [41] Ficheux, Quentin, et al. "Dynamics of a qubit while simultaneously monitoring its relaxation and dephasing." *Nature communications* 9.1 (2018): 1926.
  - [42] Cipolloni, Giorgio, and Jonah Kudler-Flam. "Non-Hermitian Hamiltonians violate the eigenstate thermalization hypothesis." *Physical Review B* 109.2 (2024): L020201.
  - [43] Jafari, R., et al. "Dynamical quantum phase transitions following a noisy quench." *Physical Review B* 109.18 (2024): L180303.
  - [44] Lavasani, Ali, Zhu-Xi Luo, and Sagar Vijay. "Monitored quantum dynamics and the Kitaev spin liquid." *Physical Review B* 108.11 (2023): 115135.
  - [45] Cao, Xiangyu, Antoine Tilloy, and Andrea De Luca. "Entanglement in a fermion chain under continuous monitoring." *SciPost Physics* 7.2 (2019): 024.
  - [46] Sriram, Adithya, et al. "Topology, criticality, and dynamically generated qubits in a stochastic measurement-only Kitaev model." *Physical Review B* 108.9 (2023): 094304.
  - [47] Wu, Wei, and Jun-Hong An. "Generalized Quantum Fluctuation Theorem for Energy Exchange." *Physical Review Letters* 133.5 (2024): 050401.
  - [48] Serbyn, Maksym, Zlatko Papi , and Dmitry A. Abanin. "Criterion for many-body localization-delocalization phase transition." *Physical Review X* 5.4 (2015): 041047.
  - [49] Chandran, A., Marc D. Schulz, and F. J. Burnell. "The eigenstate thermalization hypothesis in constrained Hilbert spaces: A case study in non-Abelian anyon chains." *Physical Review B* 94.23 (2016): 235122.
  - [50] Kim, Hyungwon, and David A. Huse. "Ballistic spreading of entanglement in a diffusive nonintegrable system." *Physical*

- review letters 111.12 (2013): 127205.
- [51] Diehl, Sebastian, et al. "Quantum states and phases in driven open quantum systems with cold atoms." *Nature Physics* 4.11 (2008): 878-883.
  - [52] Liu, Ze-Chuan, Kai Li, and Yong Xu. "Dynamical Transition Due to Feedback-Induced Skin Effect." *Physical Review Letters* 133.9 (2024): 090401.
  - [53] Xiao, Lei, et al. "Observation of non-Hermitian edge burst in quantum dynamics." *Physical Review Letters* 133.7 (2024): 070801.
  - [54] Kawabata, Kohei, et al. "Symmetry and topology in non-Hermitian physics." *Physical Review X* 9.4 (2019): 041015.
  - [55] Perrin, H., et al. "Dynamic thermalization on noisy quantum hardware." *arXiv preprint arXiv:2407.04770* (2024).
  - [56] Feng, Xu, et al. "Absence of logarithmic and algebraic scaling entanglement phases due to the skin effect." *Physical Review B* 107.9 (2023): 094309.
  - [57] Xue, Wen-Tan, et al. "Non-Hermitian edge burst." *Physical Review Letters* 128.12 (2022): 120401.
  - [58] Daley, Andrew J. "Quantum trajectories and open many-body quantum systems." *Advances in Physics* 63.2 (2014): 77-149.
  - [59] Beugeling, Wouter, Roderich Moessner, and Masudul Haque. "Off-diagonal matrix elements of local operators in many-body quantum systems." *Physical Review E* 91.1 (2015): 012144.
  - [60] Gopalakrishnan, Sarang, and Michael J. Gullans. "Entanglement and purification transitions in non-Hermitian quantum mechanics." *Physical review letters* 126.17 (2021): 170503.
  - [61] Kawabata, Kohei, Tokiro Numasawa, and Shinsei Ryu. "Entanglement phase transition induced by the non-Hermitian skin effect." *Physical Review X* 13.2 (2023): 021007.
  - [62] G. Kells, D. Meidan, and A. Romito, Topological Transitions in Weakly Monitored Free Fermions, *SciPost Phys.*14, 031 (2023).
  - [63] Buchhold, Michael, Thomas Mueller, and Sebastian Diehl. "Revealing measurement-induced phase transitions by preselection." *arXiv preprint arXiv:2208.10506* (2022).
  - [64] Schindler, Frank, et al. "Hermitian bulk–non-Hermitian boundary correspondence." *PRX Quantum* 4.3 (2023): 030315.
  - [65] Jian, Shao-Kai, et al. "Measurement-induced phase transition in the monitored Sachdev-Ye-Kitaev model." *Physical review letters* 127.14 (2021): 140601.
  - [66] Li, Yaodong, Xiao Chen, and Matthew PA Fisher. "Measurement-driven entanglement transition in hybrid quantum circuits." *Physical Review B* 100.13 (2019): 134306.
  - [67] A. Chan, R. M. Nandkishore, M. Pretko, and G. Smith, Weak measurements limit entanglement to area law (with possible log corrections), *Phys. Rev. B* 99, 224307 (2019).
  - [68] B. Skinner, J. Ruhman, and A. Nahum, Measurement-Induced Phase Transitions in the Dynamics of Entanglement, *Phys. Rev. X* 9, 031009 (2019).
  - [69] Y. Li, X. Chen, and M. P. A. Fisher, Quantum Zeno effect and the many-body entanglement transition, *Phys. Rev. B* 98, 205136 (2018).
  - [70] M. Szytniszewski, A. Romito, and H. Schomerus, Entanglement transition from variable-strength weak measurements, *Phys. Rev. B* 100, 064204 (2019).
  - [71] Manna, Sourav, Vaibhav Madhok, and Arul Lakshminarayan. "Entangling power, gate typicality and Measurement-induced Phase Transitions." *arXiv preprint arXiv:2407.17776* (2024).
  - [72] Vu, DinhDuy, and Sankar Das Sarma. "Dissipative prethermal discrete time crystal." *Physical Review Letters* 130.13 (2023): 130401.
  - [73] Ablimit, Arapat, et al. "Non-Markovian environment induced anomaly in steady state quantum coherence." *arXiv preprint arXiv:2407.03943* (2024).
  - [74] Fraenkel, Shachar, and Moshe Goldstein. "Extensive long-range entanglement at finite temperatures from a nonequilibrium bias." *Physical Review B* 110.3 (2024): 035149.
  - [75] Ashida, Yuto, and Masahito Ueda. "Full-counting many-particle dynamics: Nonlocal and chiral propagation of correlations." *Physical review letters* 120.18 (2018): 185301.
  - [76] Barch, Brian. "Locality, correlations, information, and non-Hermitian quantum systems." *Physical Review B* 110.9 (2024): 094307.
  - [77] Sala, Pablo, Jason Alicea, and Ruben Verresen. "Decoherence and wavefunction deformation of  $D_4$  non-Abelian topological order." *arXiv preprint arXiv:2409.12948* (2024).
  - [78] Lessa, Leonardo A., et al. "Strong-to-weak spontaneous symmetry breaking in mixed quantum states." *arXiv preprint arXiv:2405.03639* (2024).
  - [79] Kliesch, Martin, et al. "Locality of temperature." *Physical review x* 4.3 (2014): 031019.
  - [80] Ashida, Yuto, Keiji Saito, and Masahito Ueda. "Thermalization and heating dynamics in open generic many-body systems." *Physical review letters* 121.17 (2018): 170402.
  - [81] Chen, Yu-Hsueh, and Tarun Grover. "Separability transitions in topological states induced by local decoherence." *Physical Review Letters* 132.17 (2024): 170602.
  - [82] Shen, Tong, et al. "Disentangling the physics of the attractive Hubbard model as a fully interacting model of fermions via the accessible and symmetry-resolved entanglement entropies." *Physical Review B* 109.19 (2024): 195119.
  - [83] Skinner, Brian, Jonathan Ruhman, and Adam Nahum. "Measurement-induced phase transitions in the dynamics of entanglement." *Physical Review X* 9.3 (2019): 031009.



- [84] Chayes, Jennifer T., Lincoln Chayes, and Richard Durrett. "Critical behavior of the two-dimensional first passage time." *Journal of statistical physics* 45 (1986): 933-951.
- [85] Khasseh, Reyhaneh, et al. "Many-body synchronization in a classical Hamiltonian system." *Physical review letters* 123.18 (2019): 184301.
- [86] Willsher, Josef, et al. "Measurement-induced phase transition in a chaotic classical many-body system." *Physical Review B* 106.2 (2022): 024305.
- [87] Shirai, Tatsuhiko, and Takashi Mori. "Thermalization in open many-body systems based on eigenstate thermalization hypothesis." *Physical Review E* 101.4 (2020): 042116.
- [88] Chan, Amos, et al. "Unitary-projective entanglement dynamics." *Physical Review B* 99.22 (2019): 224307.
- [89] Li, Zhen, et al. "Observation of dynamic non-Hermitian skin effects." *Nature Communications* 15.1 (2024): 6544.
- [90] Fuji, Yohei, and Yuto Ashida. "Measurement-induced quantum criticality under continuous monitoring." *Physical Review B* 102.5 (2020): 054302.
- [91] H. M. Wiseman and G. J. Milburn, *Quantum Measurement and Control* (Cambridge University Press, Cambridge, UK, 2009).
- [92] Imbrie, John Z. "Diagonalization and many-body localization for a disordered quantum spin chain." *Physical review letters* 117.2 (2016): 027201.
- [93] Reimann, Peter. "Foundation of statistical mechanics under experimentally realistic conditions." *Physical review letters* 101.19 (2008): 190403.
- [94] Corps, Ángel L., and Armando Relaño. "General theory for discrete symmetry-breaking equilibrium states in quantum systems." *Physical Review E* 110.3 (2024): 034137.
- [95] Alsallom, Faisal, et al. "Fate of the non-Hermitian skin effect in many-body fermionic systems." *Physical Review Research* 4.3 (2022): 033122.
- [96] Knap, Michael. "Entanglement production and information scrambling in a noisy spin system." *Physical Review B* 98.18 (2018): 184416.
- [97] Rowlands, Daniel A., and Austen Lamacraft. "Noisy coupled qubits: Operator spreading and the Fredrickson-Andersen model." *Physical Review B* 98.19 (2018): 195125.
- [98] Xu, Shenglong, and Brian Swingle. "Locality, quantum fluctuations, and scrambling." *Physical Review X* 9.3 (2019): 031048.
- [99] Eisler, Viktor. "Crossover between ballistic and diffusive transport: the quantum exclusion process." *Journal of Statistical Mechanics: Theory and Experiment* 2011.06 (2011): P06007.
- [100] Amir, Ariel, Yoav Lahini, and Hagai B. Perets. "Classical diffusion of a quantum particle in a noisy environment." *Physical Review E—Statistical, Nonlinear, and Soft Matter Physics* 79.5 (2009): 050105.
- [101] T. Rakovszky, F. Pollmann, and C. W. von Keyserlingk, *Diffusive Hydrodynamics of Out-of-Time-Ordered Correlators with Charge Conservation*, *Phys. Rev. X* 8, 031058 (2018).
- [102] Cheng, Jiong, et al. "Robust fermionic-mode entanglement of a nanoelectronic system in non-Markovian environments." *Physical Review A* 91.2 (2015): 022328.
- [103] Cai, Cheng-Yun, Li-Ping Yang, and C. P. Sun. "Threshold for nonthermal stabilization of open quantum systems." *Physical Review A* 89.1 (2014): 012128.
- [104] Stefanini, Martino, and Jamir Marino. "Orthogonality catastrophe beyond bosonization from post-selection." *Physical Review Research* 6.4 (2024): L042022.
- [105] Corman, Laura, et al. "Quantized conductance through a dissipative atomic point contact." *Physical Review A* 100.5 (2019): 053605.
- [106] Xie, YuZheng, Andrew Hardy, and Arun Paramekanti. "Orbital selective order and Z<sub>3</sub> Potts nematicity from a non-Fermi liquid." *Physical Review B* 110.16 (2024): 165158.
- [107] Lane, Thomas LM, Miklós Horváth, and Kristian Patrick. "Extended edge modes and disorder preservation of a symmetry-protected topological phase out of equilibrium." *Physical Review B* 110.16 (2024): 165139.
- [108] Barontini, Giovanni, et al. "Controlling the dynamics of an open many-body quantum system with localized dissipation." *Physical review letters* 110.3 (2013): 035302.
- [109] Zhang, Zimo, et al. "Realizing Exceptional Points by Floquet Dissipative Couplings in Thermal Atoms." *Physical Review Letters* 133.13 (2024): 133601.
- [110] Fux, Gerald E., et al. "Entanglement–nonstabilizerness separation in hybrid quantum circuits." *Physical Review Research* 6.4 (2024): L042030.
- [111] Leone, Lorenzo, Salvatore FE Oliviero, and Alioscia Hama. "Stabilizer rényi entropy." *Physical Review Letters* 128.5 (2022): 050402.
- [112] Dolgirev, Pavel E., et al. "Non-Gaussian correlations imprinted by local dephasing in fermionic wires." *Physical Review B* 102.10 (2020): 100301.
- [113] Lu, Tsung-Cheng, Timothy H. Hsieh, and Tarun Grover. "Detecting topological order at finite temperature using entanglement negativity." *Physical Review Letters* 125.11 (2020): 116801.
- [114] Hastings, Matthew B. "Topological order at nonzero temperature." *Physical review letters* 107.21 (2011): 210501.
- [115] Cucchietti, Fernando M., Juan Pablo Paz, and Wojciech H. Zurek. "Decoherence from spin environments." *Physical Review A—Atomic, Molecular, and Optical Physics* 72.5 (2005): 052113.
- [116] Tamascelli, Dario, et al. "Nonperturbative treatment of non-Markovian dynamics of open quantum systems." *Physical*

- review letters 120.3 (2018): 030402.
- [117] Wang, He-Ran, Xiao-Yang Yang, and Zhong Wang. "Exact Hidden Markovian Dynamics in Quantum Circuits." *Physical Review Letters* 133.17 (2024): 170402.
  - [118] Wang, Han-Yi, et al. "Interrelated thermalization and quantum criticality in a lattice gauge simulator." *Physical Review Letters* 131.5 (2023): 050401.
  - [119] Buchhold, M., et al. "Effective theory for the measurement-induced phase transition of Dirac fermions." *Physical Review X* 11.4 (2021): 041004.
  - [120] Gopalakrishnan, Sarang, K. Ranjibul Islam, and Michael Knap. "Noise-induced subdiffusion in strongly localized quantum systems." *Physical review letters* 119.4 (2017): 046601.
  - [121] Will, Melissa, Roderich Moessner, and Frank Pollmann. "Realization of Hilbert Space Fragmentation and Fracton Dynamics in Two Dimensions." *Physical Review Letters* 133.19 (2024): 196301.
  - [122] Corman, Laura, et al. "Quantized conductance through a dissipative atomic point contact." *Physical Review A* 100.5 (2019): 053605.
  - [123] Popkov, Vladislav, and Roberto Livi. "Manipulating energy and spin currents in non-equilibrium systems of interacting qubits." *New Journal of Physics* 15.2 (2013): 023030.
  - [124] De, Ayush, et al. "Stochastic sampling of operator growth dynamics." *Physical Review B* 110.15 (2024): 155135.
  - [125] Zhang, Hao, and Alex Kamenev. "Anatomy of topological Anderson transitions." *Physical Review B* 108.22 (2023): 224201.
  - [126] Bohrdt, Annabelle, et al. "Scrambling and thermalization in a diffusive quantum many-body system." *New Journal of Physics* 19.6 (2017): 063001.
  - [127] Klocke, Kai, Joel E. Moore, and Michael Buchhold. "Power-Law Entanglement and Hilbert Space Fragmentation in Nonreciprocal Quantum Circuits." *Physical Review Letters* 133.7 (2024): 070401.
  - [128] Alberton, Ori, Michael Buchhold, and Sebastian Diehl. "Entanglement transition in a monitored free-fermion chain: From extended criticality to area law." *Physical Review Letters* 126.17 (2021): 170602.
  - [129] Loio, Hugo, et al. "Purification timescales in monitored fermions." *Physical Review B* 108.2 (2023): L020306.
  - [130] Cao, Kui, Qian Du, and Su-Peng Kou. "Many-body non-Hermitian skin effect at finite temperatures." *Physical Review B* 108.16 (2023): 165420.
  - [131] Sahu, Himanshu. "Information scrambling in quantum walks: Discrete-time formulation of Krylov complexity." *Physical Review A* 110.5 (2024): 052405.
  - [132] Aziz Alaoui, Youssef, et al. "Measuring Bipartite Spin Correlations of Lattice-Trapped Dipolar Atoms." *Physical Review Letters* 133.20 (2024): 203401.
  - [133] Cai, Zi, and Thomas Barthel. "Algebraic versus exponential decoherence in dissipative many-particle systems." *Physical review letters* 111.15 (2013): 150403.
  - [134] Nandy, Sourav, et al. "Reconstructing effective Hamiltonians from nonequilibrium thermal and prethermal steady states." *Physical Review Research* 6.2 (2024): 023160.
  - [135] Cipolloni, Giorgio, and Jonah Kudler-Flam. "Entanglement entropy of non-Hermitian eigenstates and the Ginibre ensemble." *Physical Review Letters* 130.1 (2023): 010401.
  - [136] Le Gal, Youenn, Xhek Turkeshi, and Marco Schirò. "Entanglement dynamics in monitored systems and the role of quantum jumps." *PRX Quantum* 5.3 (2024): 030329.
  - [137] Landi, Gabriel T., et al. "Current fluctuations in open quantum systems: Bridging the gap between quantum continuous measurements and full counting statistics." *PRX Quantum* 5.2 (2024): 020201.
  - [138] Li, Yaodong, Xiao Chen, and Matthew PA Fisher. "Quantum Zeno effect and the many-body entanglement transition." *Physical Review B* 98.20 (2018): 205136.
  - [139] Turkeshi, Xhek, and Marco Schirò. "Entanglement and correlation spreading in non-Hermitian spin chains." *Physical Review B* 107.2 (2023): L020403.
  - [140] Roscilde, Tommaso, et al. "Scalable spin squeezing from critical slowing down in short-range interacting systems." *Physical Review Letters* 133.21 (2024): 210401.
  - [141] Ueda, Masahito. "Nonequilibrium open-system theory for continuous photodetection processes: A probability-density-functional description." *Physical Review A* 41.7 (1990): 3875.
  - [142] Choi, Soonwon, et al. "Observation of discrete time-crystalline order in a disordered dipolar many-body system." *Nature* 543.7644 (2017): 221-225.
  - [143] Roscilde, Tommaso, Tommaso Comparin, and Fabio Mezzacapo. "Entangling dynamics from effective rotor-spin-wave separation in U (1)-symmetric quantum spin models." *Physical Review Letters* 131.16 (2023): 160403.
  - [144] Dora, Balazs, Doru Sticlet, and Catalin Paşcu Moca. "Correlations at PT-symmetric quantum critical point." *Physical Review Letters* 128.14 (2022): 146804.
  - [145] Abanin, Dmitry A., Wojciech De Roeck, and François Huveneers. "Exponentially slow heating in periodically driven many-body systems." *Physical review letters* 115.25 (2015): 256803.
  - [146] Li, Jia-Kun, et al. "Photonic simulation of Majorana-based Jones polynomials." *Physical Review Letters* 133.23 (2024): 230603.
  - [147] Wu, Chen-Huan. "Non-defective degeneracy in non-Hermitian bipartite system." *Physica Scripta* 99.10 (2024): 105237.
  - [148] Scarlatella, Orazio, et al. "Dynamical mean-field theory for markovian open quantum many-body systems." *Physical Review X* 11.3 (2021): 031018.

- [149] Chen, Qianqian, Shuai A. Chen, and Zheng Zhu. "Weak ergodicity breaking in non-Hermitian many-body systems." *SciPost Physics* 15.2 (2023): 052.
- [150] Mondaini, Rubem, and Marcos Rigol. "Eigenstate thermalization in the two-dimensional transverse field Ising model. II. Off-diagonal matrix elements of observables." *Physical Review E* 96.1 (2017): 012157.
- [151] Znidaric, Marko. "Solvable quantum nonequilibrium model exhibiting a phase transition and a matrix product representation." *Physical Review E—Statistical, Nonlinear, and Soft Matter Physics* 83.1 (2011): 011108.
- [152] Shiratani, Sora, and Synge Todo. "Stochastic parameter optimization analysis of dynamical quantum critical phenomena in the long-range transverse-field Ising chain." *Physical Review E* 110.6 (2024): 064106.
- [153] Roscilde, Tommaso, Tommaso Comparin, and Fabio Mezzacapo. "Entangling dynamics from effective rotor–spin-wave separation in U (1)-symmetric quantum spin models." *Physical Review Letters* 131.16 (2023): 160403.
- [154] Adler, Daniel, et al. "Observation of Hilbert space fragmentation and fractonic excitations in 2D." *Nature* (2024): 1-6.
- [155] Calabrese, Pasquale, John Cardy, and Erik Tonni. "Entanglement negativity in quantum field theory." *Physical review letters* 109.13 (2012): 130502.
- [156] Bennett, Charles H., et al. "Concentrating partial entanglement by local operations." *Physical Review A* 53.4 (1996): 2046.
- [157] Prosen, Tomaž, and Marko Žnidarič. "Long-range order in nonequilibrium interacting quantum spin chains." *Physical review letters* 105.6 (2010): 060603.
- [158] Jin, Tony, and David G. Martin. "Measurement-induced phase transition in a single-body tight-binding model." *Physical Review B* 110.6 (2024): L060202.
- [159] Poboiko, Igor, et al. "Theory of free fermions under random projective measurements." *Physical Review X* 13.4 (2023): 041046.
- [160] Ali, T., Bhattacharyya, A., Haque, S. S., Kim, E. H., Moynihan, N., & Murugan, J. (2020). Chaos and complexity in quantum mechanics. *Physical Review D*, 101(2), 026021.
- [161] Zhu, Qingling, et al. "Observation of thermalization and information scrambling in a superconducting quantum processor." *Physical Review Letters* 128.16 (2022): 160502.
- [162] Iyoda, Eiki, and Takahiro Sagawa. "Scrambling of quantum information in quantum many-body systems." *Physical Review A* 97.4 (2018): 042330.
- [163] Yin, Ruoyu, et al. "Restart uncertainty relation for monitored quantum dynamics." *Proceedings of the National Academy of Sciences* 122.1 (2025): e2402912121.
- [164] Turkeshi, Xhek, Lorenzo Piroli, and Marco Schiró. "Enhanced entanglement negativity in boundary-driven monitored fermionic chains." *Physical Review B* 106.2 (2022): 024304.
- [165] Kelly, Shane P., and Jamir Marino. "Entanglement transitions induced by quantum-data collection." *Physical Review A* 111.1 (2025): L010402.
- [166] Block, Maxwell, et al. "Measurement-induced transition in long-range interacting quantum circuits." *Physical Review Letters* 128.1 (2022): 010604.
- [167] Piilo, Jyrki, et al. "Non-Markovian quantum jumps." *Physical review letters* 100.18 (2008): 180402.
- [168] Passarelli, Gianluca, et al. "Many-body dynamics in monitored atomic gases without postselection barrier." *Physical Review Letters* 132.16 (2024): 163401.
- [169] Shammah, Nathan, et al. "Open quantum systems with local and collective incoherent processes: Efficient numerical simulations using permutational invariance." *Physical Review A* 98.6 (2018): 063815.
- [170] Wang, Ting-Tung, et al. "Entanglement microscopy and tomography in many-body systems." *Nature Communications* 16.1 (2025): 96.
- [171] Solanki, Parvinder, et al. "Exotic synchronization in continuous time crystals outside the symmetric subspace." *Physical Review Letters* 133.26 (2024): 260403.
- [172] Turner C Jet al 2018 Weak ergodicity breaking from quantum many-body scars *Nat. Phys.* 14 745–9
- [173] Pausch, Lukas, et al. "How to seed ergodic dynamics of interacting bosons under conditions of many-body quantum chaos." *arXiv preprint arXiv:2501.13556* (2025).
- [174] Muzzi, Cristiano, Mikheil Tsitsishvili, and Giuliano Chiriacò. "Entanglement enhancement induced by noise in inhomogeneously monitored systems." *Physical Review B* 111.1 (2025): 014312.
- [175] Andersen, Trond I., et al. "Thermalization and criticality on an analogue–digital quantum simulator." *Nature* 638.8049 (2025): 79–85.
- [176] Santos, Lea F., Anatoli Polkovnikov, and Marcos Rigol. "Entropy of isolated quantum systems after a quench." *Physical review letters* 107.4 (2011): 040601.
- [177] Basit, Abdul, et al. "Interplay between nonequilibrium and non-Markovianity in controlling the entropic uncertainty bound." *Physical Review A* 110.1 (2024): 012429.
- [178] Settimo, Federico, Heinz-Peter Breuer, and Bassano Vacchini. "Entropic and trace-distance-based measures of non-Markovianity." *Physical Review A* 106.4 (2022): 042212.
- [179] Majtey, Ana P., Pedro W. Lamberti, and Domingo P. Prato. "Jensen-Shannon divergence as a measure of distinguishability between mixed quantum states." *Physical Review A—Atomic, Molecular, and Optical Physics* 72.5 (2005): 052310.
- [180] Kumar Chauhan, Anil, A. Kani, and Jason Twamley. "Enhancing macroscopic multimode entanglement through many-body interactions in cavity magnomechanics." *Physical Review A* 111.3 (2025): 033505.

- [181] Varikuti, Naga Dileep, and Soumik Bandyopadhyay. "Unraveling the emergence of quantum state designs in systems with symmetry." *Quantum* 8 (2024): 1456.
- [182] Garratt, Samuel J., and Max McGinley. "Entanglement and private information in many-body thermal states." *arXiv preprint arXiv:2502.13218* (2025).
- [183] Shapourian, Hassan, and Shinsei Ryu. "Entanglement negativity of fermions: Monotonicity, separability criterion, and classification of few-mode states." *Physical Review A* 99.2 (2019): 022310.
- [184] Pati, Arun Kumar, Uttam Singh, and Urbasi Sinha. "Measuring non-Hermitian operators via weak values." *Physical Review A* 92.5 (2015): 052120.